Geological Society of America Bulletin

Age and regional tectonic implications of Late Cretaceous thrusting and Eocene extension, Cabinet Mountains, northwest Montana and northern Idaho

JEFFREY A. FILLIPONE and AN YIN

Geological Society of America Bulletin 1994;106, no. 8;1017-1032
doi: 10.1130/0016-7606(1994)106<1017:AARTIO>2.3.CO;2

Age and regional tectonic implications of Late Cretaceous thrusting and Eocene extension, Cabinet Mountains, northwest Montana and northern Idaho

JEFFREY A. FILLIPONE
AN YIN
Department of Earth and Space Sciences, University of California, Los Angeles, California 90024-1567

ABSTRACT

Understanding the kinematic and temporal relationships between the Cordilleran magmatic belt and the foreland fold and thrust belt can provide insights into the development of thrust systems in retro-arc settings. Combining data from field mapping and $^{40}Ar/^{39}Ar$ geochronometry and thermochronometry, we show that Late Cretaceous thrusting in the Cabinet Mountains of the northwest Montana thrust belt coincided both spatially and temporally with hinterland magmatism. Thrusting and magmatism in the hinterland of the northwest and southwest Montana thrust belt were coeval with development of the foreland fold and thrust belt during the Late Cretaceous. Movement on the Moyie thrust, a principal thrust in the western part of the Purcell anticlinorium, occurred between ca. 71 and 69 Ma. In the Cabinet Mountains, the anticlinorium developed by systems of east- and west-directed thrusts, with a southward decrease in slip on the Moyie thrust that helped contribute to less overall shortening in the anticlinorium in Montana than in British Columbia. The lithosphere underlying the anticlinorium may have been thermally weakened by magmatic heating, promoting the development of both the Late Cretaceous thrusts and early to middle Eocene normal faults.

INTRODUCTION

The Cordilleran orogen from the southern Andes to Alaska developed during a lengthy and complex period of convergence between dominantly oceanic plates of Pacific affinity and continental lithosphere. Along this belt, continental crust was affected by repeated episodes of shortening and arc magmatism. Uncertainties remain, however, as to whether magmatism caused thrusting, what the sequence of thrusting was, and how thrusting in the hinterland was related kinematically and temporally to that in the foreland. Theories developed to explain the relationship between magmatism and thrusting in the Cordillera have included displacement by magma (Smith, 1981; Scholten, 1973; Allmendinger and Jordan, 1981) and thermal weakening by magmatic heating (Burchfiel and Davis, 1975; Scholten, 1982; Isacks, 1988). Each theory embodies a set of predictions for the development of structures across the orogen that can be tested by observations. In the North American foreland fold and thrust belt, it has been proposed that (1) magmatism and thrusting were synchronous (Hyndman and others, 1988), (2) that magmatism caused thrusting (Smith, 1981), and (3) that magmatism was a result of anatexis due to crustal thickening (Archibald and others, 1984). Some or all of these proposals may be mutually compatible. Interpretation of how magmatism and thrusting were related also has important implications for palinspastic reconstruction of the fold and thrust belt (for example, Allmendinger and Jordan, 1981).

In the northwest United States and southwest Canada, the eastern Cordillera consists of a magmatic belt of Mesozoic to early Tertiary age in the west, transitional with the foreland fold and thrust belt to the east. Unlike the example of the Cenozoic Andes, the transition between the magmatic belt and the foreland fold and thrust belt is well exposed in northwest Montana and southeast British Columbia, providing a glimpse into deeper structural levels of the hinterland. In an effort to understand the relationship between magmatism and thrusting, we address the following questions: what are the relative ages of magmatism and thrusting, what sequence did thrusting follow in the hinterland-foreland transition, and how did the transition zone between the foreland and hinterland, now occupied by the Purcell anticlinorium, evolve during this time? Price (1981) and Archibald and others (1984) have shown that some east-directed thrusts are "stitched" by Cretaceous plutons in the Purcell anticlinorium. These thrusts thus are apparently older than in southwestern Montana where magmatism and thrusting overlapped in both space and time (Robinson and others, 1968).

Mapping of crosscutting relations and $^{40}Ar/^{39}Ar$ geochronometry and thermochronometry in the Cabinet Mountains place limits on the ages of magmatism and thrusting in the hinterland. In this paper, we discuss local deformation related to pluton emplacement, geometry and kinematics of thrusts, and associated structures and ages of plutonism and deformation. We conclude that the fold and thrust belt in this region experienced synmagmatic east- and west-directed thrusting in the Late Cretaceous. Inferred ages of thrusting from the eastern part of the Montana fold and thrust belt suggest that synchronous thrusting took place between the hinterland and foreland at that time. The regional décollement, into which all major thrusts are interpreted to root, formed a throughgoing thrust system beneath the Purcell anticlinorium, linking regions of coeval shortening in the foreland and hinterland. These findings are consistent with many predictions of thrust timing and geometry deduced from mechanical models of thrusting (Elliott, 1976; Chapple, 1978; Davis and others, 1983; Platt, 1986; Yin, 1993). During the middle to late Eocene, the thrust belt was dismantled along northwest-striking normal faults (Hope and Rock Lake faults) and east-dipping detachment

Data Repository item 9415 contains additional material related to this article.

Geological Society of America Bulletin, v. 106, p. 1017–1032, 15 figs., 2 tables, August 1994.

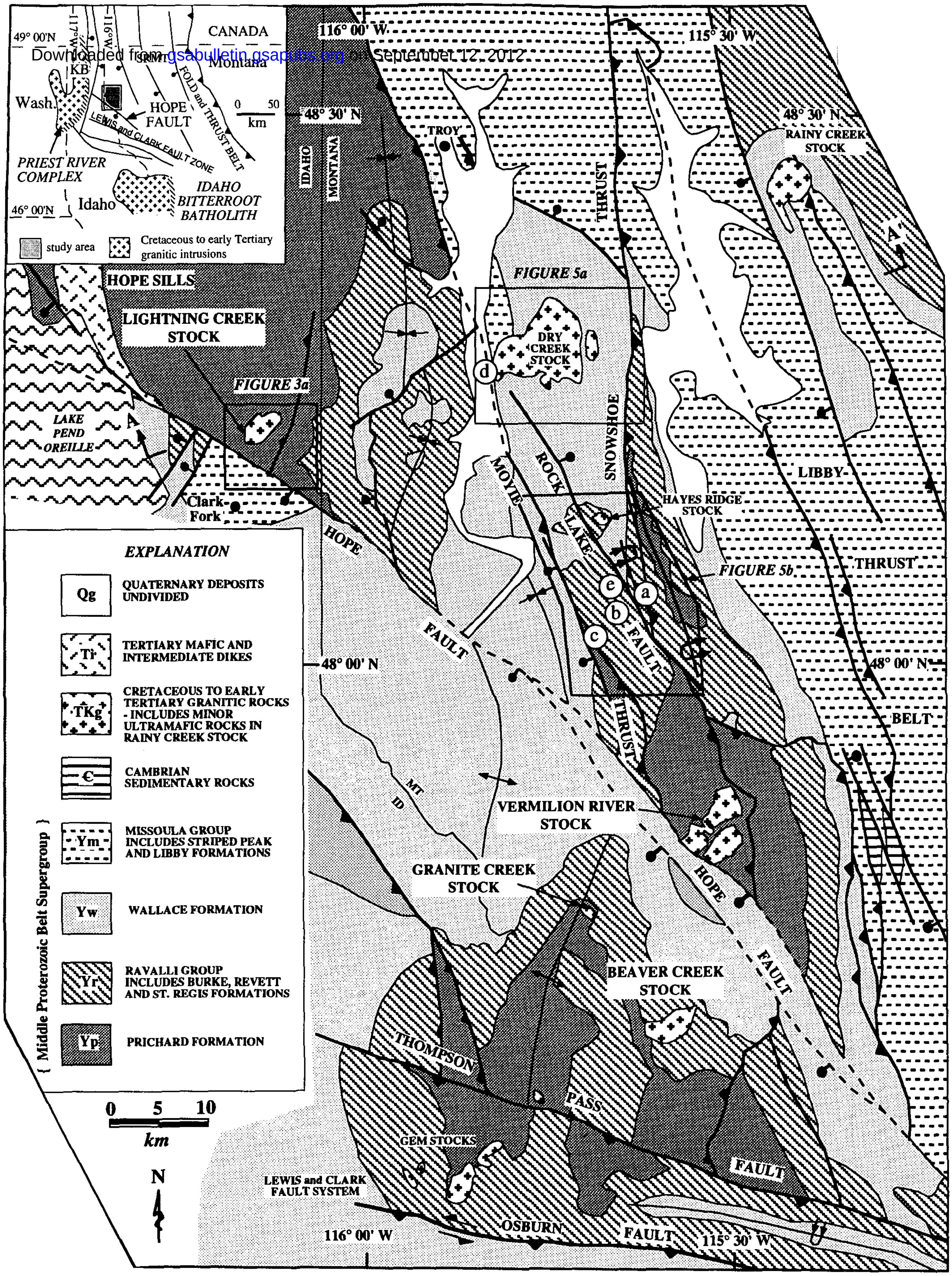

49° 00'N
CANADA
Montana
KB
Wash.
HOPE
FAULT
LEWIS and CLARK FAULT ZONE
FOLD and THRUST BELT
0 50
km
PRIEST RIVER
COMPLEX
IDAHO
BITTERROOT
BATHOLITH
46° 00'N
Idaho
study area
Cretaceous to early Tertiary granitic intrusions
116° 00' W
115° 30' W
48° 30' N
48° 30' N
TROY
IDAHO
MONTANA
THRUST
RAINY CREEK
STOCK
FIGURE 5a
HOPE SILLS
LIGHTNING CREEK
STOCK
DRY
CREEK
STOCK
FIGURE 3a
LAKE
PEND
OREILLE
A
A'
MOYIE
ROCK
SNOWSHOE
LAKE
LIBBY
HAYES RIDGE
STOCK
Clark
Fork
HOPE
FIGURE 5b
THRUST
FAULT
FAULT
48° 00' N
48° 00' N
THRUST
BELT
EXPLANATION
Qg QUATERNARY DEPOSITS UNDIVIDED
Ti TERTIARY MAFIC AND INTERMEDIATE DIKES
TKg CRETACEOUS TO EARLY TERTIARY GRANITIC ROCKS - INCLUDES MINOR ULTRAMAFIC ROCKS IN RAINY CREEK STOCK
Є CAMBRIAN SEDIMENTARY ROCKS
Middle Proterozoic Belt Supergroup
Ym MISSOULA GROUP INCLUDES STRIPED PEAK AND LIBBY FORMATIONS
Yw WALLACE FORMATION
Yr RAVALLI GROUP INCLUDES BURKE, REVETT AND ST. REGIS FORMATIONS
Yp PRICHARD FORMATION
MT
ID
VERMILION RIVER
STOCK
GRANITE CREEK
STOCK
HOPE
FAULT
BEAVER CREEK
STOCK
THOMPSON
PASS
FAULT
GEM STOCKS
LEWIS and CLARK
FAULT SYSTEM
OSBURN
FAULT
116° 00' W
115° 30' W
0 5 10
km
N

faults associated with metamorphic core complexes.

TECTONIC SETTING

The Cabinet Mountains form the western flank of the Purcell anticlinorium in the northern U.S. Rocky Mountains (Fig. 1). The anticlinorium is a regional structural culmination cored by rocks of the Belt Supergroup and extends from southeast British Columbia through the Cabinet Mountains and into the northern margin of the Idaho (Bitterroot) batholith. The Purcell trench, a major physiographic trough at the western limit of the anticlinorium, has been interpreted as the site of detachment faulting along low-angle normal faults that translated hanging-wall rocks in the Cabinet Mountains eastward from footwall rocks of the Priest River metamorphic complex in the Idaho Selkirk Mountains during the early Tertiary (Rehrig and others, 1987; Rhodes and Hyndman, 1984; Harms and Price, 1992). Although the pre-extensional structural configuration of the region is uncertain, Belt and younger rocks cut by east-directed thrust faults can be identified west of the Priest River complex (Rhodes and Hyndman, 1988; Stoffel and others, 1991), suggesting that the thrust belt extended as far west as the Kootenay Arc in Washington. Continuity, however, between thrusts west of the Priest River complex and those in the Cabinet Mountains has not been established.

Discussions of the geometry and structural style of thrusting in the Cabinet Mountains have been presented by Harrison and others (1980, 1986), Harrison and Cressman (1985), Wells and others (1981), and Yoos and others (1991), yet controversy still exists as to whether this region is underlain by a thin-skinned or basement-involved thrust system (see summary by Yoos and others, 1991).

Figure 1. Generalized geologic map of the Cabinet Mountains, northwest Montana and northeast Idaho, adapted from Harrison and others (1972, 1986, 1992), Gibson (1948), and Wells and others (1981), with additional field mapping from this study. Location of maps in Figures 3a and 5 also are indicated. Localities mentioned in the text are (a) Rock Lake, (b) Rock Peak, (c) Rock Creek, (d) Bull Lake Valley, (e) St. Paul Pass. Inset is a tectonic sketch map with the location of the study area. KB stands for the Kaniksu batholith, which is part of the Priest River Complex. Diagonal pattern represents the mylonitized parts of the batholiths.

STRATIGRAPHY

The Cabinet Mountains constitute the westernmost part of the Cordilleran foreland fold and thrust belt and are almost entirely underlain by Middle Proterozoic Belt Supergroup (Fig. 2). The Belt strata consist of fine-grained siliciclastic and carbonate rocks that locally are intruded by relatively small (10–60 km^2), granitic plutons of late Mesozoic to early Tertiary age (Fig. 1). Sparse exposures of Cambrian and Tertiary sedimentary rocks are also present (Harrison and others, 1986, 1992; Bush, 1989). Different interpretations of Belt stratigraphy in the region complicate the placing of contacts between these mostly transitional formations (see Winston, 1986, for regional correlations of Belt strata). Consequently, the thicknesses of formations we report are estimated from mapping and cross sections and may not match exactly those reported by others (for example, Harrison and others, 1986; Wells and others, 1981). The oldest unit in the study area is the Prichard Formation, or lowermost Belt, which is overlain by the Ravalli Group comprising the Burke, Revett, and St. Regis Formations. The Wallace Formation, also known as the "middle Belt carbonate," overlies the Ravalli Group and is succeeded by the Striped Peak Formation, the youngest formation in the map area. A lack of adequate exposures and gradational contacts prevented us from making finer subdivisions of the Belt stratigraphy.

As much as 10,000 m of Prichard Formation has been estimated from exposures in the Sylvanite anticline to the north (Harrison and Cressman, 1985), but only 520 m were observed in the Cabinet Mountains by Wells and others (1981). As the base of the Prichard Formation is nowhere exposed, we have assumed a minimum thickness of 4 km (Harrison and others, 1986) to 7.6 km (Harrison and others, 1992). The Prichard Formation consists mainly of dark gray to black and white striped argillite, siltite, and silty argillite with thin beds of light gray quartzite. It characteristically weathers an orange or rust color attributable to the pervasive presence of pyrite and pyrrhotite. Numerous mafic sills, either of demonstrated or inferred Middle Proterozoic age, intrude throughout the Prichard Formation (Harrison and others, 1992). Winston (1989) suggested that sedimentary structures are useful for interpreting the Belt stratigraphy. We found this especially effective in placing the contact between the Prichard and Burke Formations. The contact between the Prichard and the Burke Formation is placed where thinly parallel-laminated, dark gray to black siltite grades into medium to dark gray, wavy laminated, locally cross-bedded siltite. The Burke Formation passes upward from gray wavy-laminated, lenticularly bedded siltite with abundant sole marks, into pale gray quartzite and silty quartzite in the upper few hundred meters of the formation. We mapped 1,520 m of the Burke Formation near Rock Peak (Fig. 1, location b), equivalent to the 1,500 m estimated by Wells and others (1981). The Revett Formation is mostly me-

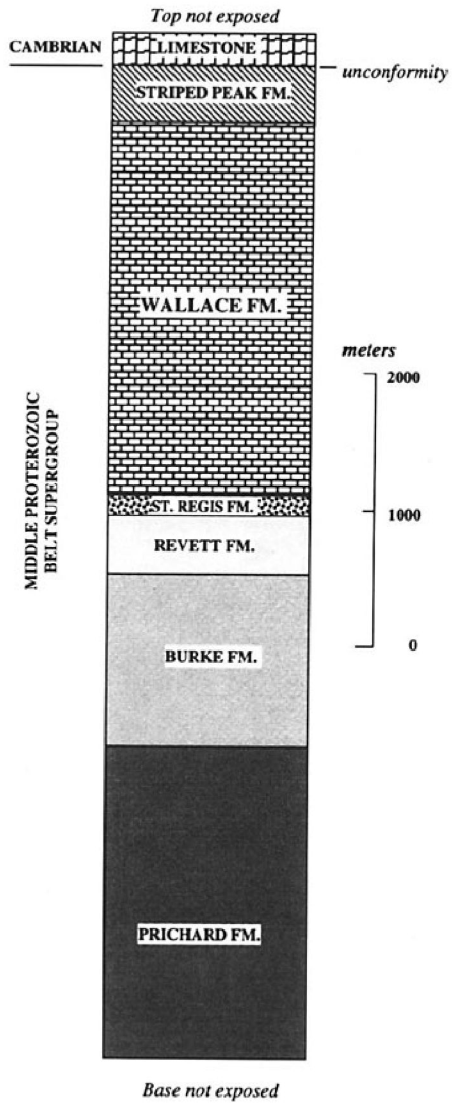

Figure 2. Stratigraphic column of Belt Supergroup rocks in the Cabinet Mountains, northwest Montana. Thicknesses are taken from mapping in this study and published sources (Harrison and others, 1986, 1992; Wells and others, 1981).

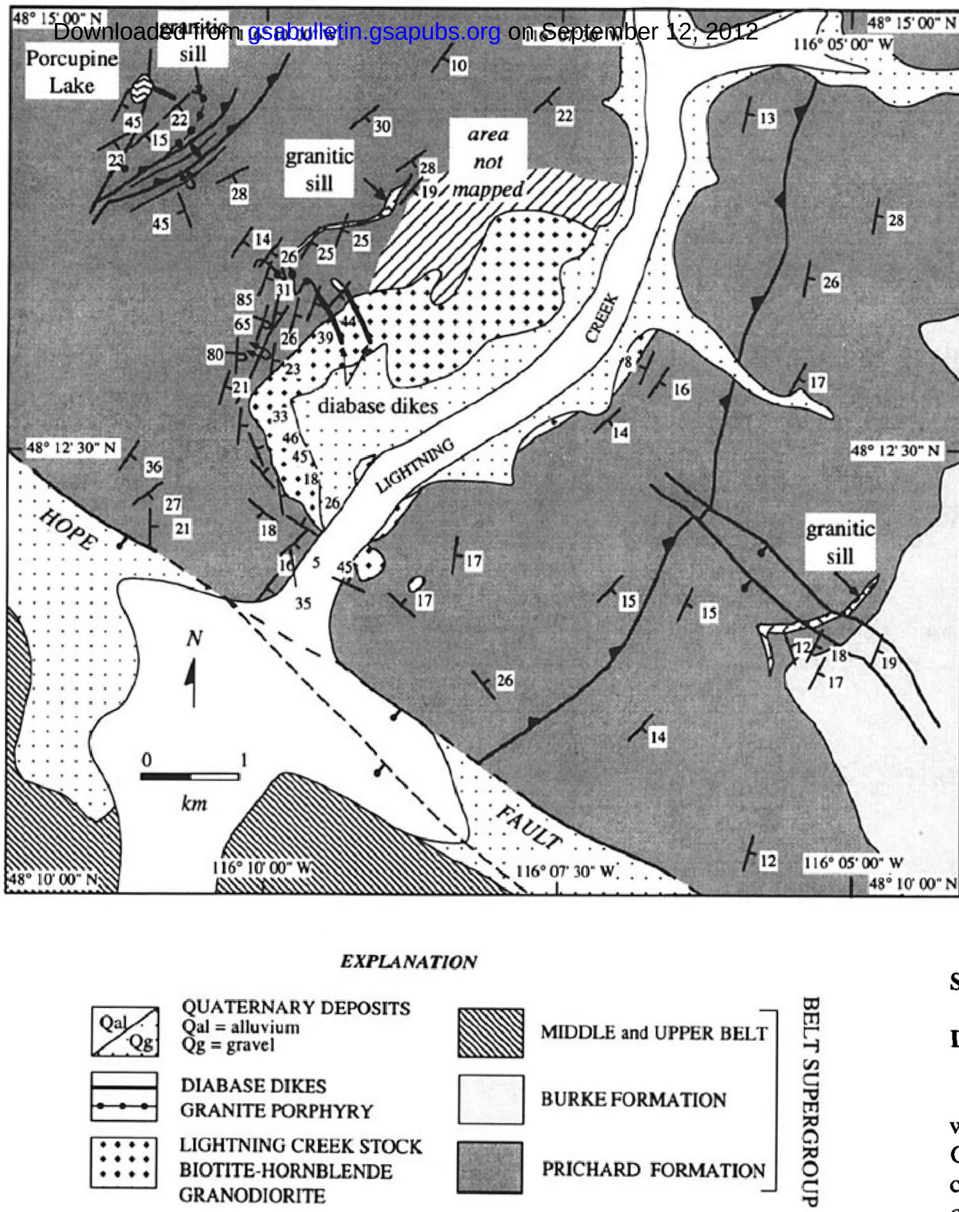

Figure 3. Geologic map of the Lightning Creek stock and vicinity. Strong deflection of bedding has occurred adjacent to the stock. Bedding attitudes north and east of the stock and distribution of Quaternary deposits are from Harrison and Jobin (1963).

dium grained, light gray to whitish quartzite and silty quartzite in its lower part, with distinctive large-scale (0.5–1.0 m high) planar cross-beds, grading upward into siltite, minor carbonate, and argillite of the St. Regis Formation. Thickness of the Revett Formation near Rock Peak is about 500 m. The St. Regis Formation is dominated by gray dolostone and fissile, dark-green to gray shaly argillite with minor siltite. Thickness of the formation is about 200 m on the east side of the Cabinet Mountains, where one of only a few unfaulted exposures is found. The Wallace Formation is the highest stratigraphic unit we mapped. Harrison and others (1986, 1992) divided it into lower, middle, and upper parts; we mapped only the lower and middle parts of the Formation. The lower part consists mostly of dark gray to green-gray fissile argillite in gradational contact with the St. Regis Formation, passing upward into dark gray argillite and dolostone that weathers buff to pale orange. The middle Wallace Formation consists of siltite, argillite, and intermittent gray dolostone. Combined thickness of the lower and middle Wallace in the region is about 2,800 m (Harrison and others, 1986). The Striped Peak Formation overlies the Wallace Formation in the northern Cabinet Mountains, occurring in several areas surrounding the Dry Creek stock (Fig. 1). We did not map extensively in this formation.

STRUCTURAL GEOLOGY

Deformation Adjacent to Plutons

Several prominent granitoid plutons with well-developed contact aureoles occur in the Cabinet Mountains. Ductile deformation of country rocks was locally significant in the contact aureoles, which host moderate to high-temperature and low-pressure mineral assemblages (for example, andalusite, muscovite, biotite, zoisite). Besides ductile folding, mapping of bedding and minor folds around the Dry Creek and Lightning Creek stocks (Fig. 1) shows that deformation of bedding occurred as much as 0.5 to 1.5 km away from the plutons. Steepening of beds against the walls of the Lightning Creek stock (Fig. 3) occurred with little associated folding, whereas ductile similar-style folds are common in the contact aureole of the Dry Creek stock. The style of deformation near the Lightning Creek stock resembles the "return flow" predicted by Marsh (1982). Contacts of both plutons with their country rocks are sharp, with little apparent infolding of country rocks into the plutons. We inter-

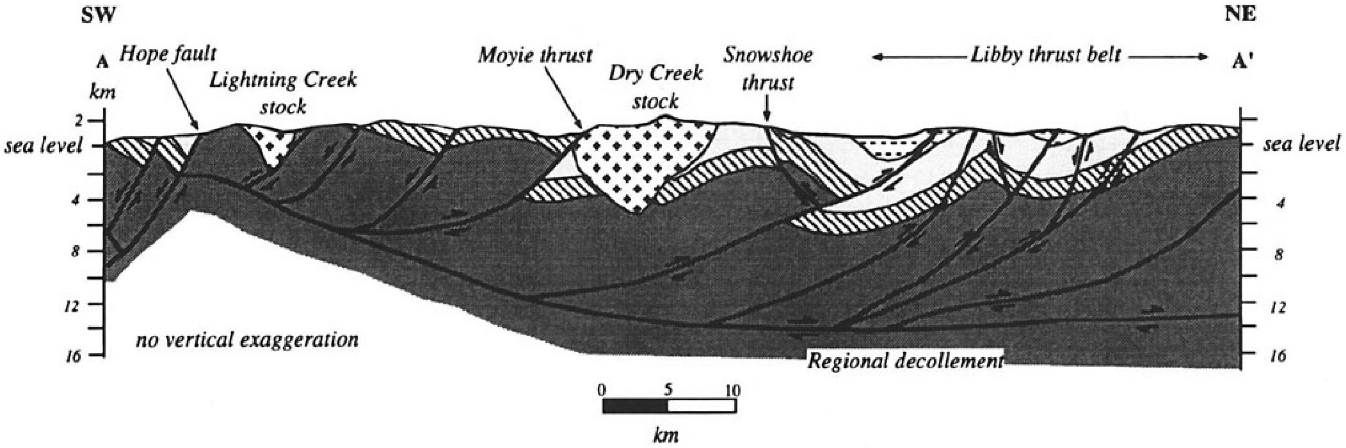

Figure 4. Cross section A–A′ through the central Cabinet Mountains (see Fig. 1 for location). Major imbricate thrust faults occur in the Moyie and Snowshoe thrust systems and the Libby thrust belt. The basal décollement is placed on the basis of bed-length balancing and the depth to décollement of Harrison and Cressman (1985) and Harrison and others (1992) for the Libby thrust belt. The Snowshoe thrust is interpreted to merge with the Libby thrust, but other plausible explanations are discussed in the text.

pret the observed deformation as having developed during the final stages of pluton emplacement.

East-directed Thrust Systems

Harrison and Cressman (1985) first described the Libby thrust belt (LTB) that lies ~15 km east of the Cabinet Mountains (Fig. 1). The LTB consists of a series of east-directed thrust faults that may sole into a basal décollement in Belt strata at a depth of at least 15 km (Harrison and Cressman, 1985; and Fig. 4). About 20 km west of the Libby thrust belt, a second major east-directed thrust, the Moyie thrust, places middle and lower Belt on middle and upper Belt strata (Fig. 1). The Moyie thrust previously was identified as a major thrust in the northwest Montana and southeast British Columbia foreland fold and thrust belt (Price, 1981; McMechan and Price, 1982). The Moyie thrust probably roots into the same décollement as the LTB, making the Libby and Moyie thrusts part of the same east-directed thrust system (Fig. 4; see also Harrison and others, 1992).

Structures in the footwall of the Moyie thrust include mylonitic foliation in granitic rocks (Dry Creek stock) and discrete faulting associated with development of foliation and brecciation of Belt rocks. The deformed western margin of the Dry Creek stock provides some of the best evidence for the effects of shearing and age of movement on the Moyie thrust (Fig. 1, location d, and Fig. 5a). A small outcrop of inferred Prichard Formation in Bull Lake Valley is juxtaposed against the Striped Peak Formation, making the stratigraphic throw at this location the greatest observed in the map area. Harrison and others (1992) showed Prichard Formation thrust over the Libby Formation near Troy, Montana (see Fig. 1). The Moyie thrust also is exposed in the Rock Creek area, south of the Dry Creek stock (Fig. 1, location c, and Fig. 4), where it juxtaposes Prichard Formation in the hanging wall over Revett Formation in the footwall. Thicknesses of Belt strata compiled from Gibson (1948), Wells and others (1981), and the regional cross section in Figure 4 indicate 4 ± 0.5 km of dip slip along the Moyie thrust in the central Cabinet Mountains. This is substantially less than the ~8 km interpreted by McMechan and Price (1982) for the Moyie thrust in southeast British Columbia. At Rock Creek, the western part of the Moyie thrust plate is truncated by a later down-to-the-west normal fault (Fig. 5b), juxtaposing lower Wallace Formation against Prichard Formation, and creating a fault-bounded cross-sectional "wedge" of the Prichard Formation (Wells and others, 1981; see Fig. 5b, location 4, and Fig. 6a).

At this locality, Prichard Formation in the thrust sheet has a strongly developed spaced to slaty cleavage containing pervasive mineral elongation lineations. Cleavage orientations vary between 320°–345°/20°–60°SW, with mineral lineations oriented ~220°/40°–70° (Fig. 7a). Also present are minor fault surfaces containing stretched minerals and striations (minor faults = 330°–350°/45°–80°SW; striations = 220°–250°/30°–55°; Fig. 7b) that are consistent with cleavage and mineral lineations. We interpret both sets of lineations as the projections of the maximum stretch in the fault plane and approximate net slip direction of the Moyie thrust. Greater shortening strain of rocks inside the wedge compared to those outside is indicated by the local transposition of bedding and cleavage in the wedge.

Mylonitic Granite Along the Moyie Thrust

The Dry Creek stock is deformed along its western margin by the Moyie thrust. The trace of the Moyie thrust lies in Bull Lake Valley, where it is covered by glacial gravel and alluvium (Fig. 1, location d). However, shallowly southwest-dipping shear surfaces (C-surfaces) and foliation (S-surfaces) that form a composite S-C mylonitic fabric (Berthe and others, 1979) are well exposed along the east side of the valley.

The mesoscopic C-surfaces are expressed geomorphically as northwest-striking dip slopes along a series of east-trending truncated spurs along the eastern side of Bull Lake Valley (Gibson, 1948). The schistosity is close in strike to the C-surfaces but dips more steeply southwestward. The schistosity consists of medium- to fine-grained biotite and muscovite anastamosing around planar to sigmoidal aggregates of quartz and feldspar (Fig. 8a). K-feldspar augen, common in the mylonite, have locally undergone grain-size reduction by fracturing. C-surfaces have a consistent spacing of 2–5 mm and make angles of 30°–40° with S-surfaces. A moderately to well-developed stretching lineation composed of elongated quartz grains, along with the angle created by the two planar fabrics, provides shear sense indicators (Simpson and Schmid, 1983; Choukroune and others, 1987) that indicate consistent top-to-the-northeast shear along the Moyie thrust (Fig. 8b).

The mylonitic fabric can be categorized as Type II S-C fabric in the classification of Lister and Snoke (1984) because of the preferred development of C-surfaces over S-surfaces and the presence of abundant kinked and sigmoidal muscovite crystals. The fabric meets Paterson and others' (1989) criteria for solid-state fabrics that postdate pluton emplacement and crystallization. Solid-state deformation is consistent with the contrast between crystallization and fabric ages determined by U-Pb and $^{40}Ar/^{39}Ar$ dating discussed below.

West-directed Structures—The Snowshoe Thrust System

Intervening between the dominant east-directed Moyie and Libby thrust systems is the west-directed Snowshoe thrust system (Figs. 5b and 6b). Known formerly as the Snowshoe fault (Gibson, 1948; Wells and others, 1981), and shown as an east-directed thrust by Harrison and others (1992), these faults have been identified by us as rare examples of west-directed thrusts in the Montana thrust belt. The regional distribution of west-verging structures in the southeastern Canadian Cordillera is reviewed and discussed by Price (1986).

The main Snowshoe thrust can be traced from the southeast Cabinet Mountains northward for at least 100 km, from Rock Lake to the British Columbia–Montana boundary (Fig. 1; see also Harrison and others, 1992). The slip direction of the thrust as defined by striations on fault surfaces (Fig. 9) plunges 45°–50° toward 065°–070°, on a moderately dipping fault surface (strike/dip = 340°–350°/45°–65°NE). Shortening across this thrust varies from a few hundred meters near Rock Lake (Fig. 6a), to 4 ± 1 km in the northeast Cabinet Mountains (Fig. 4). We mapped a related low-angle thrust, the Libby Lakes thrust (R. Franklin, personal commun., 1991), in the footwall of the Snowshoe thrust, about 1–1.5 km structurally below the main fault (Figs. 6a and 6b). The southward decrease in displacement on the Snowshoe thrust near Rock Lake is due, in part, to displacement transfer from the Snowshoe to the Libby Lakes thrust. East of Rock Lake, cumulative displacement on these two faults is about 1 km. A system of closely spaced imbricate west-directed thrusts that repeats the Burke and Revett Formations occurs in a

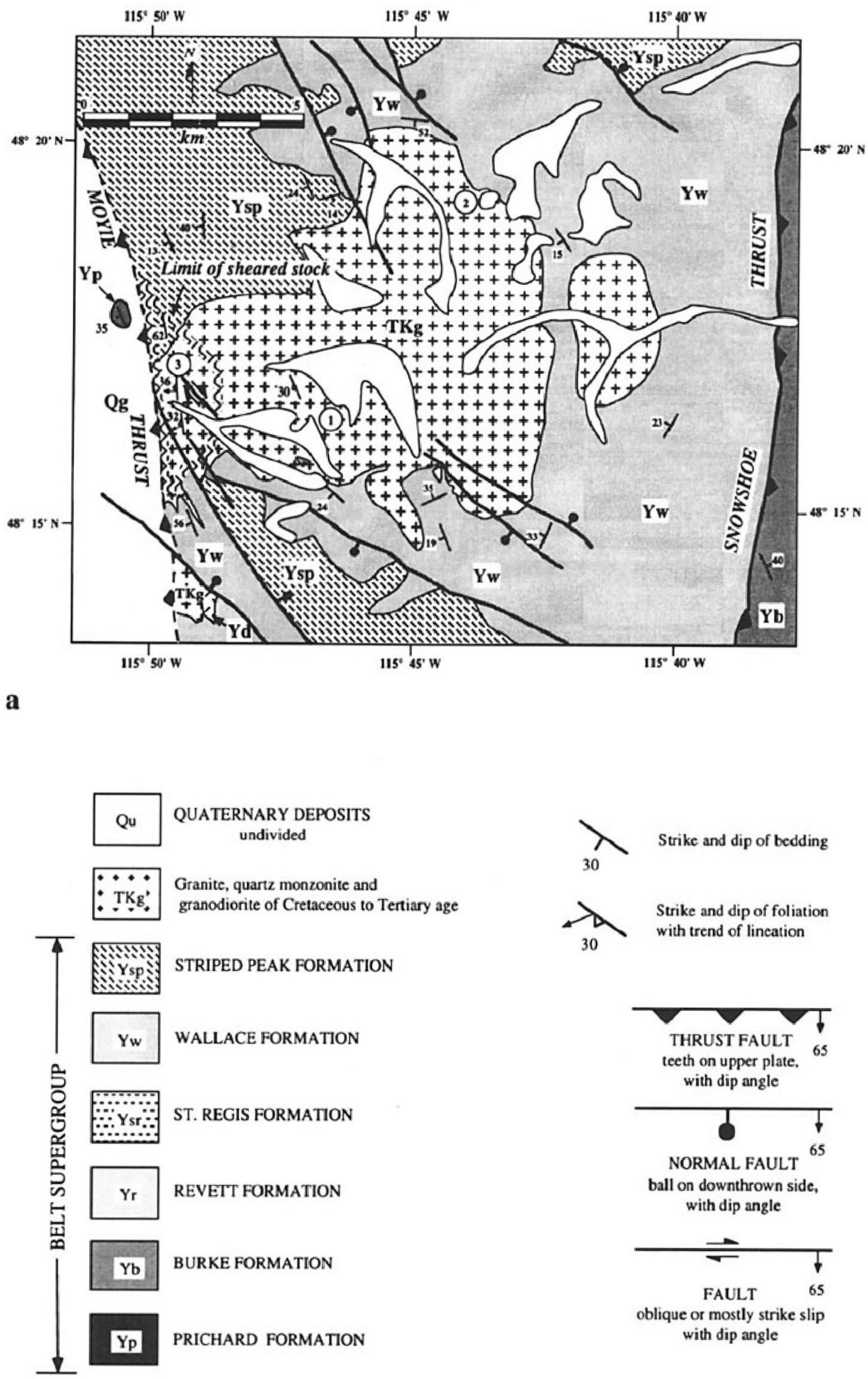

Figure 5. Geologic maps of the (a) Dry Creek stock and surrounding area and (b) the Rock Lake area. Map symbols include bedding with dip angle; thrust faults—teeth on upper plate; normal faults—ball on downthrown side; Yd = diorite of probable Precambrian age. In a, samples discussed in text are indicated by numbered locations: 1 = sample DC-10; 2 = sample DC-57; 3 = sample DC-26. In b, locations are 1 = Rock Lake; 2 = Isabella Lake; 3 = St. Paul Pass; 4 = Rock Creek; EPA = Elephant Peak anticline. Locations of cross sections B–B′ and C–C′ (Fig. 6) are indicated. Stars are the locations where kinematic data from thrusts were gathered (data presented in Fig. 9). Both maps incorporate supplementary data on location of contacts from Wells and others (1981).

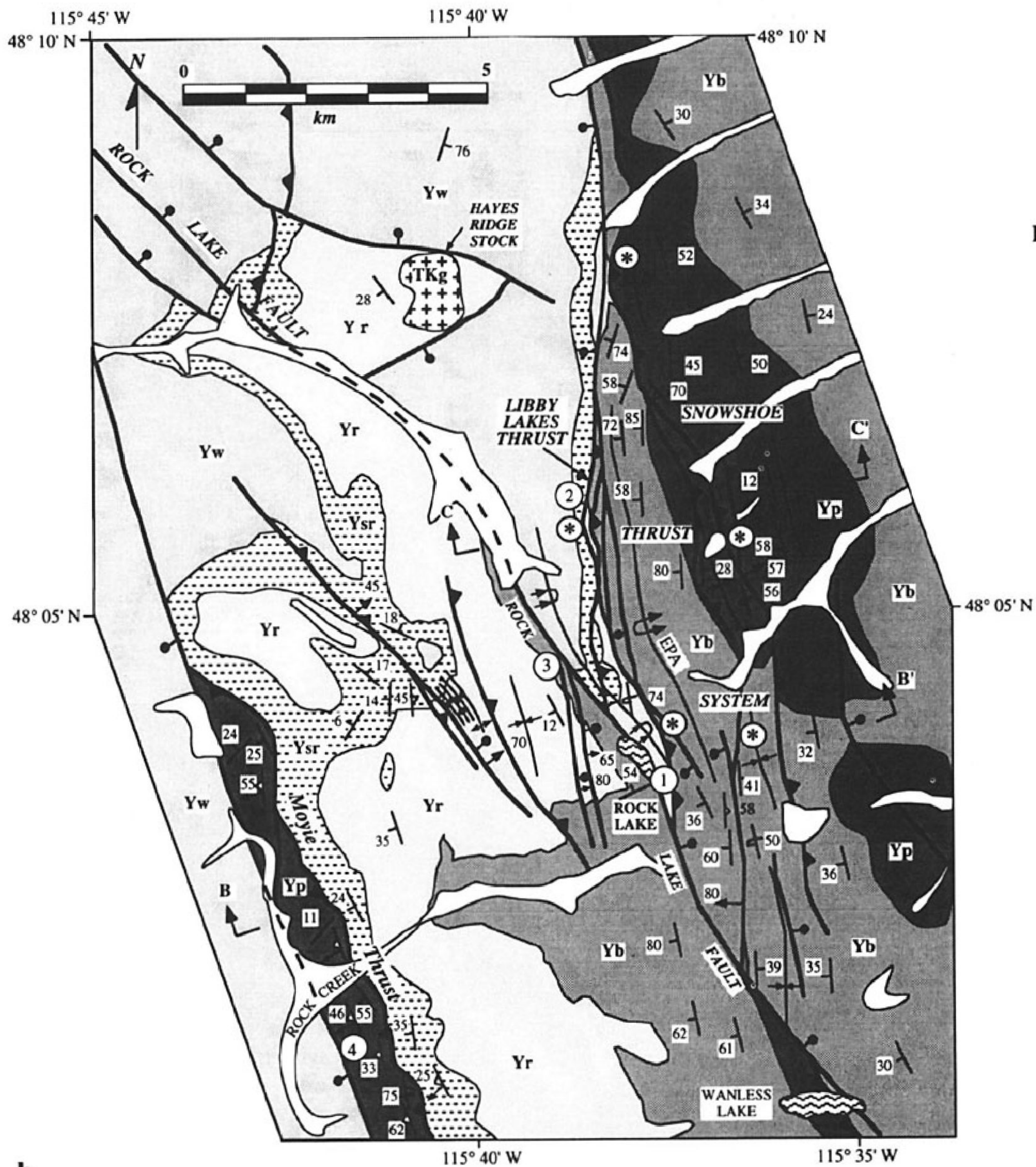

b

Figure 5. (*Continued*).

zone within 1 km below the main strand of the southern part of the Snowshoe thrust and appears to be the northward continuation of the Libby Lakes thrust (Figs. 5b, 6b, and 10a). Minor bedding-parallel normal faults on the steep, nearly vertical west-facing limb of the Elephant Peak anticline (Figs. 6a, 6b, and 10b) offset the Libby Lakes thrust and west-verging folds. West-directed thrusts are not recognized south of Wanless Lake (Fig. 5b) where the west-verging folds merge with northeast-verging folds (Gibson, 1948; Harrison and others, 1986).

West-verging Folds and Axial Planar Cleavage

Associated with the imbricate thrusts are large-scale (~3- to 5-km wavelength) asymmetric folds that are overturned toward the west (Figs. 6b and 10c). Axial planar spaced cleavage dips at shallow angles eastward, producing a strong intersection lineation with bedding (Fig. 11). The range of cleavage orientations (320°–015°/20°–80°NE) and steepening of the cleavage and lineations in the Rock Lake area are attributed to movement on the Rock Lake fault (Fig. 5b). Mapping the cleavage and lineations helps delineate the relative ages of the east- and west-directed structures. East-dipping fabrics when traced westward in the Rock Lake area are abruptly overlain by west-dipping fabrics in the hanging wall of the Moyie thrust (Fig. 5b, location 4). The juxtaposition of west-dipping cleavage in the Moyie thrust sheet over the east-dipping cleavage near Rock Creek suggests that emplacement of the Moyie thrust sheet postdated development of the Snowshoe thrust and associated structures. About 4 km

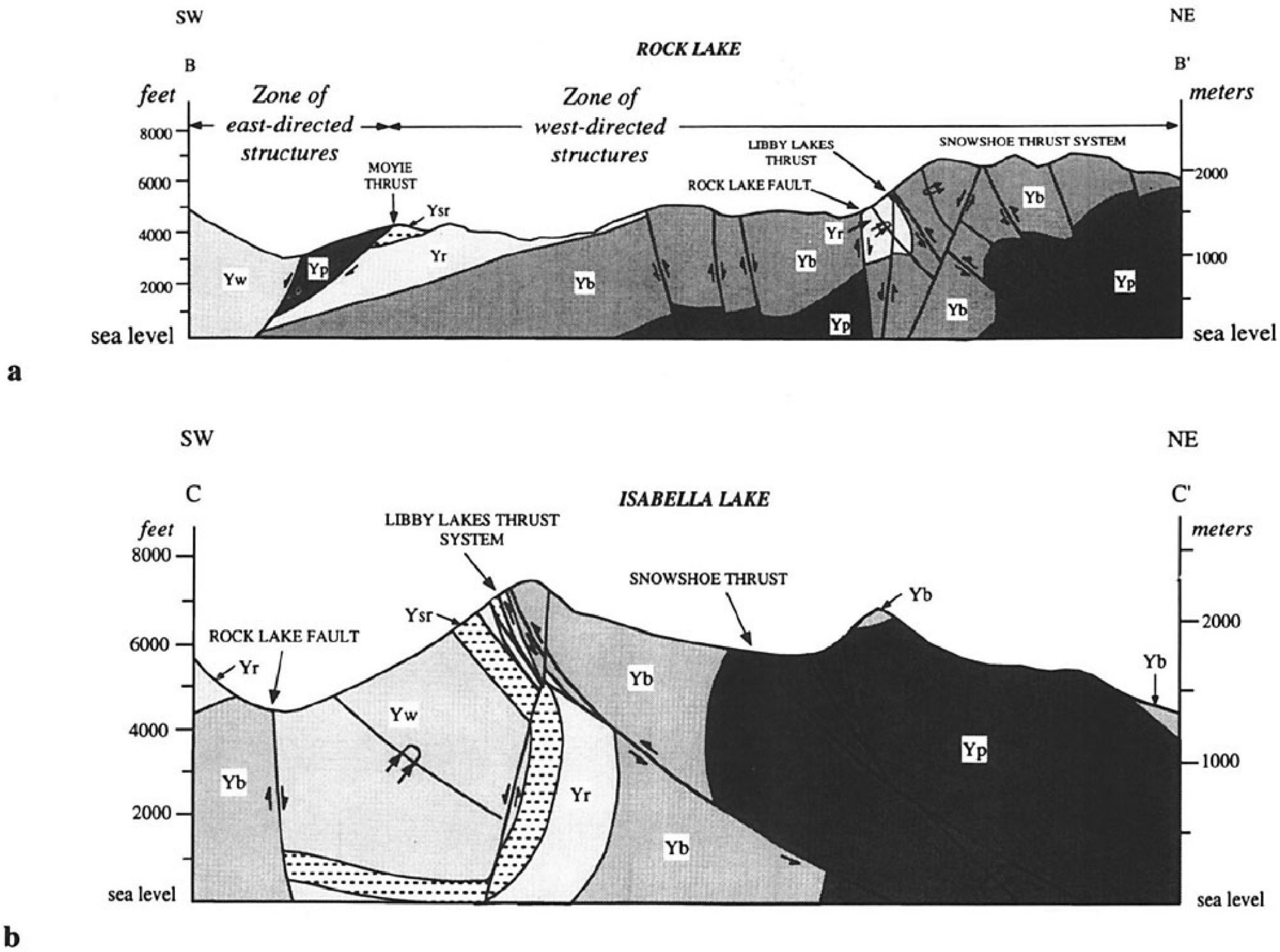

Figure 6. (a) Cross section through the Rock Lake area that includes the Libby Lakes and Snowshoe thrusts and the fault-bounded wedge of Prichard Formation in the hanging wall of the Moyie thrust. Zones of west- and east-directed structures are indicated. (b) Cross section through the Isabella Lake area illustrating west-directed imbricate thrusts of the Libby Lakes and Snowshoe thrust systems, cut by later bedding-plane parallel normal faults. See Figure 5 for explanation of symbols.

southeast of Rock Lake, the Moyie thrust truncates west-verging folds and fabrics of the Snowshoe thrust system (Harrison and others, 1986), indicating that the Snowshoe thrust sheet there was also overridden by the Moyie thrust sheet.

The relative age and slip direction of the Snowshoe thrust suggest that the east-directed thrust system comprises two parts: an upper plate (Moyie) above the Snowshoe thrust, and a lower plate (LTB) below the Snowshoe thrust (Fig. 4). Despite its relatively small displacement, the along-strike continuity and west-directed displacement of the Snowshoe thrust suggest that it played an important kinematic role in the development of the western Purcell anticlinorium. West-directed structures are a prominent element of the regional structural geometry in the southeast Canadian Cordillera (Price, 1986), where they are spectacularly developed in the Selkirk Fan structure (Brown and Tippet, 1978). In western Montana and northern Idaho, most of these are developed adjacent to, or between, plutons (Gwinn, 1961; Harrison and Schmidt, 1971). The presence of these structures in the hinterland but not farther into the foreland suggests that synthrusting magmatism and metamorphism may promote the development of this structural style.

Downdip projection of the Snowshoe thrust indicates that it must encounter the Libby thrust. Thus, the Snowshoe thrust is expected either to have a crosscutting relationship with the Libby thrust or to merge with it. Without any subsurface information on the Snowshoe thrust, cross sections constructed from surface geology are the only means to assess its geometry at depth. Two plausible options for the age and kinematic role of the Snowshoe thrust with respect to the LTB and the Moyie thrust are (1) that the Snowshoe thrust is a backthrust to the east-directed LTB/Moyie thrust system or (2) that it postdates those east-directed thrusts (Fig. 12). Regardless of which is correct, some degree of hindward imbrication is evident, suggesting emplacement of the Moyie thrust sheet late in the thrusting history of the Cabinet Mountains.

Rock Lake Fault

The Rock Lake fault is a north-northwest–striking fault, with a highly variable but generally steep dip, that juxtaposes younger Belt rocks on the east against older Belt rocks on the west (Fig. 5b). The fault crosscuts west-directed structures related to the Snowshoe thrust, making it a younger feature. The

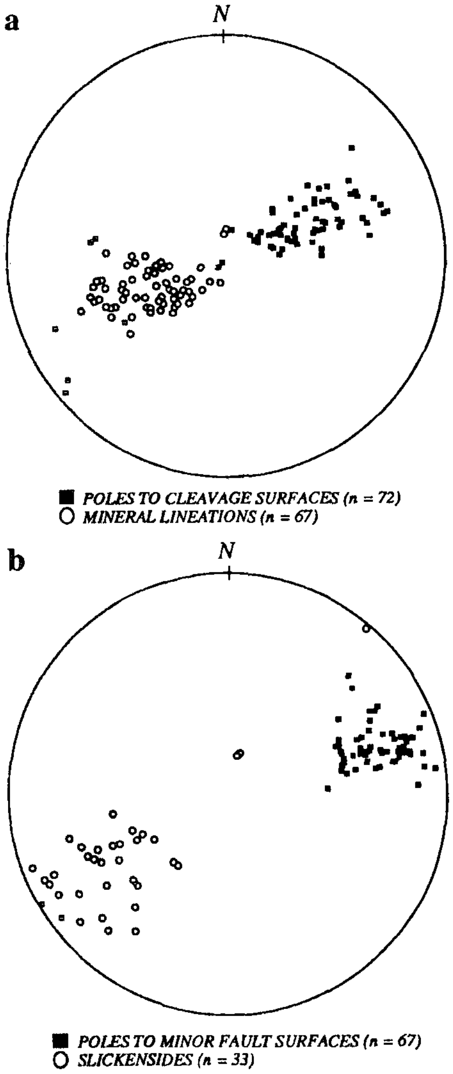

Figure 7. Structural and kinematic data from the fault-bounded thrust "wedge" of Prichard Formation, hanging wall of the Moyie thrust: (a) west-dipping cleavage and mineral elongation lineations and (b) minor faults and lineations defined by fibrous quartz and slickenside striae.

Rock Lake fault offsets a major sedimentary-hosted Cu-Ag deposit near Rock Lake (Figs. 5b and 6b); one of a number of such deposits in the Revett Formation of northwest Montana and adjacent Idaho (Lange and Sherry, 1983).

The fault zone is 2 to 5 m wide where exposed and contains strongly striated fine-grained breccia and clay gouge. The abundance of veins and fragmented wall rocks in the fault zone attests to the brittle nature of the presently exposed level of the fault. Filled extension gashes indicative of dilation across the fault zone are present as much as 50 m from the main fault trace. Several other northerly striking, *en echelon* down-to-the-east minor normal faults lie in the footwall of the Hope fault, making an angle of about 20° with the strike of the Rock Lake fault (Fig. 5b). Kinematics of the Rock Lake fault were documented at several locations in the Rock Lake area. Where exposed, the fault has an orientation of 165°–185°/70°–90°E (Fig. 13). Fault plane striations (Fig. 13) and slickensides have a broad range of orientations (100°–150°/35°–80°), but beds show a consistent down-to-the-southeast sense of offset, notwithstanding the possibility of multiple episodes of movement.

Two locations were mapped where west-verging folds and west-directed thrusts of the Snowshoe thrust system are cut by the Rock Lake fault (Figs. 5b, 6a, and 6b). East-dipping cleavage axial-planar to west-verging folds within the Snowshoe thrust system occurs both west and east of the fault, becoming highly distorted in the vicinity of the fault. Imbricate thrusts in the footwall of the Snowshoe thrust that are cut by the Rock Lake fault near Rock Lake (Figs. 5b and 6a) have no observable offset counterparts west of the Rock Lake fault. This is probably due to uplift and subsequent erosion of the footwall of the Rock Lake fault.

A lower (older) age limit for the Rock Lake fault is provided by dating of the Hayes Ridge stock, a small two-mica granite with spectacular, large (1–4 cm across) euhedral muscovite phenocrysts, and a well-developed contact aureole that lies east of the Rock Lake fault in the central Cabinet Mountains (Fig. 5b). The stock is apparently exposed only to the east of the Rock Lake fault, suggesting that the fault cuts the Hayes Ridge stock (see geochronology section).

Hope Fault

At the south end of the Cabinet Mountains, the Moyie thrust is truncated by the Hope fault (Fig. 1). Controversial interpretations of the age and kinematics of the Hope fault have been reviewed by Yin (1991). As much as 8 ± 2 km of dip slip was estimated for the fault near Vermilion River in the southern Cabinet Mountains (Fillipone and others, 1992). This displacement must have caused substantial upward warping of the regional thrust décollement in the footwall of the Hope fault as interpreted in Figure 4. Our interpretation of the décollement contrasts with that of Harrison and others (1992), who assume crystalline basement slices above a gently west-dipping décollement in this part of the thrust belt.

GEOCHRONOLOGY AND THERMOCHRONOLOGY

$^{40}Ar/^{39}Ar$ Method

Minerals from the granitic plutons were sized at 30–60 mesh and separated using standard heavy liquid and magnetic techniques. The minerals were wrapped in Sn foil and sealed in evacuated quartz vials (6 mm I.D.) with Fish Canyon sanidine flux monitors (FC-3) at ~5-mm intervals and were irradiated for 45 h in the H-5 position of the University of Michigan Ford reactor. Sanidine crystals from the irradiated flux monitors were fused with a 5 W Ar ion laser and analyzed for their Ar isotopic compositions. J-factors were calculated from several analyses from each monitor position, using a flux monitor age of 27.8 Ma (Miller and others, 1985). Vacuum-fused K_2SO_4 and CaF_2 included in the tube were used to calculate correction factors for $(^{40}Ar/^{39}Ar)_K$, $(^{39}Ar/^{37}Ar)_{Ca}$, and $(^{36}Ar/^{37}Ar)_{Ca}$.

Samples were then step-heated in a Ta crucible in a double-vacuum furnace. Reactive gases were removed by reaction with the hot Ta crucible wall and an SAES Ti-Zr getter. Isotopic measurements were made at UCLA using a VG 1200S automated mass spectrometer operated in the electron multiplier mode. Sensitivities for these analyses ranged from 4.6×10^{-17} mol Ar/mV to 2×10^{-17} mol Ar/mV. Argon blanks over the course of the analyses averaged 1×10^{-15} mol ^{40}Ar in an atmospheric ratio. Tabulated results of the Ar isotopic analyses, uncorrected for neutron-produced interferences, are presented with calculated ages with one-sigma uncertainties.[1] Uncertainties do not include error in the J-factor, which is typically ~0.5%.

U-Pb Method

Details of the U-Pb analyses are given in Table 1. The reader is referred to Gehrels (1990) for details of the techniques used.

Electron Microprobe Analyses[2]

Analyses were performed on a Cameca Camebax in wavelength and energy dispersive mode at an accelerating voltage of 15 kV

[1]GSA Data Repository item 9415, tables of analytical data for each sample, is available on request from Documents Secretary, GSA, P.O. Box 9140, Boulder, CO 80301.

[2]Analytical data for hornblendes are available on request from the first author at the address given.

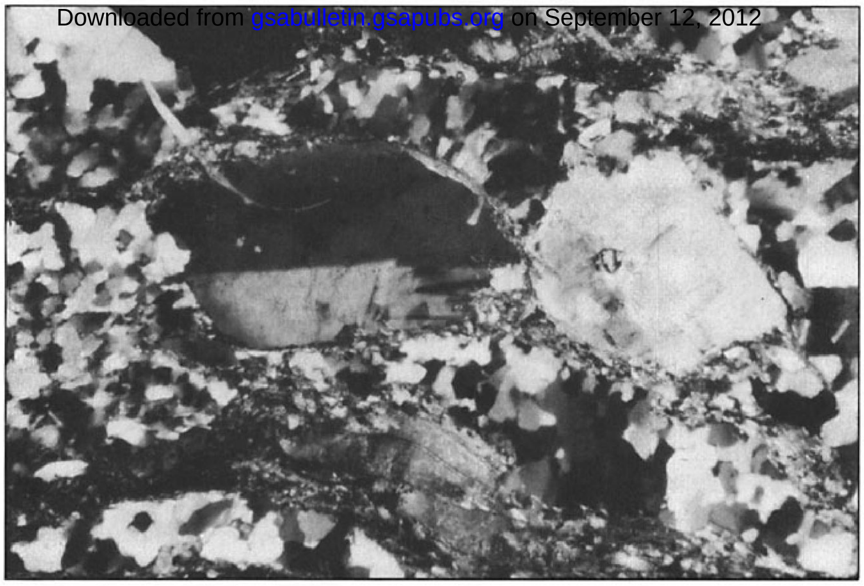

a

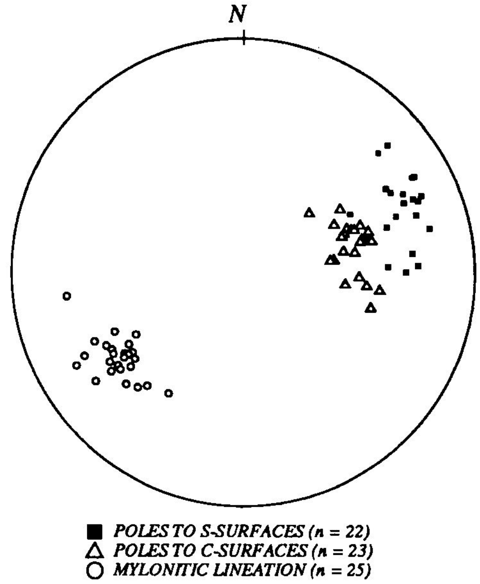

b

Figure 8. S-C mylonite along the western margin of the Dry Creek stock. (a) Photomicrograph, crossed polars. Field of view is ~5 mm across. Sense of shear is top-to-the-northeast (left). Note asymmetric tails of polygonized quartz on feldspar porphyroclasts. (b) Lower hemisphere, equal-area projection of S-C fabric data.

and with sample currents of ~10–15 nA. Natural and synthetic minerals and oxides from the UCLA collection were used as standards. ZAF corrections were applied to the raw intensities from all analyses. The limit of detectability is about ±0.02 wt% for the wavelength dispersive mode and is somewhat higher for the energy dispersive model. Sources of error include known precisions of standard element concentrations, ZAF correction accuracies, machine drift, and counting statistics. Counting errors were maintained at <1% for the standards (counting time = 20 s). Analytical results were in general reproducible within about 2% error.

RESULTS

Age of the Moyie Thrust and Dry Creek Stock

Age of the Moyie thrust has been established by dating the Dry Creek stock, which is cut by the Moyie thrust. The stock has well-developed solid-state shear fabrics only along its western margin adjacent to the Moyie thrust; the rest of the outer and interior parts of the pluton is undeformed. At the northwest edge of the sheared stock we also mapped minor fault surfaces and brecciated zones in Striped Peak argillite (Fig. 5a).

$^{40}Ar/^{39}Ar$ and U-Pb zircon dating and hornblende barometry from the undeformed part of the pluton provide data on the age and depth of emplacement and a lower (older) age limit on the time of thrusting. Most of the $^{40}Ar/^{39}Ar$ age spectra are somewhat complex, involving plateau and smoothly varying segments or complex age gradients. For consistency, we have interpreted these as simply as possible in conjunction with our geologic observations. A U-Pb zircon date for the undeformed pluton (sample DC-10, Fig. 5a) does not fully agree with the $^{40}Ar/^{39}Ar$ data. A concordia plot of the data (Fig. 14) shows strong discordance with a lower intercept age of 74.1 ± 7.3 Ma and significant inherited components with an average age of ~1,680 Ma. Biotite from this sample yielded a $^{40}Ar/^{39}Ar$ apparent age of ~64.5 ± 1 Ma, corresponding to 82% of the gas released (Fig. 15a)[3]. A $^{40}Ar/^{39}Ar$ hornblende age spectrum for a second sample from the undeformed stock (sample DC-57, Fig. 5a) is saddle-shaped, with a minimum age of 85 ± 0.2 Ma and a total gas age of 93.9 Ma (Fig. 15b). Biotite from DC-57 has a relatively flat age spectrum (Fig. 15b) that gives an apparent age of ~71.4 ± 0.9 Ma for 99.4% of the gas released. Wells and others (1981) dated microcline and biotite from an unspecified part of the Dry Creek stock by the Rb-Sr method, yielding a two-point "isochron" with an age of 71 ± 2 Ma (recalculated using new decay constants; Z. Peterman, personal commun., 1990). The contrast between the $^{40}Ar/^{39}Ar$ and U-Pb zircon dates for the Dry Creek stock may suggest that either (1) the intrusive history spanned a period of at least 12 m.y. (if errors in both samples are applied to minimize their age difference) or (2) the apparent age difference between these two sample localities, separated by 6 km, implies separate intrusive phases of the pluton. Consistently younger ages from sample DC-10 than for DC-57 suggest two intrusive phases. Furthermore, the U-Pb date comes from a petrologically similar, but hornblende-free part of the pluton. Biotite age spectra from the two samples suggest that cooling below the closure temperature of biotite occurred at different times for different parts of the pluton. The extremely high Sr initial ratio noted by Wells and others (1981) may reflect a disturbance of isotope systematics rendering the Rb-Sr date suspect.

A second granitic pluton that lies in the footwall of the principal branch of the Moyie thrust, the Vermilion River stock (Fig. 1), is older than the Dry Creek stock, with a $^{40}Ar/^{39}Ar$ hornblende plateau age of 113.7 ± 1.5 Ma for 75.2% gas released (Fig. 15c). Harrison and others (1986) concluded that this plu-

[3]Age is calculated by weighting the individual model ages that form apparent plateaus according to their percent ^{39}Ar released. Error reported is 1 s.d. for the weighted age only and does not include the precision on ages of individual steps.

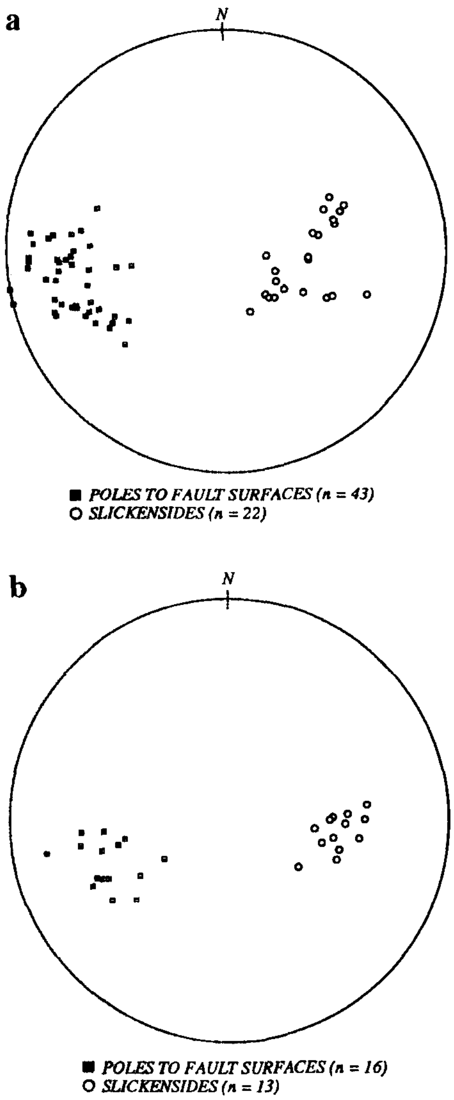

Figure 9. Lower hemisphere equal-area projection of kinematic data from (a) the Snowshoe thrust and (b) the Libby Lakes thrust; locations where data were collected are indicated by stars in Figure 5b.

ton crosscuts the Moyie thrust. This is inconsistent, as discussed below, with the age that we have determined for the Moyie thrust. A third pluton composed of hornblende-biotite granodiorite, the Lightning Creek stock, lies in the upper Prichard Formation west of the Moyie thrust (Fig. 3a). Step heating results of hornblende and biotite from this pluton yielded $^{40}Ar/^{39}Ar$ apparent ages of 75.7 ± 0.9 Ma (85.1% gas released) and 71.4 ± 0.7 Ma (plateau age, 93.4% gas released) for hornblende and biotite, respectively (Fig. 15d).

We used the aluminum-in-hornblende geobarometer of Johnson and Rutherford (1989) to estimate pressures, and thus depths of crystallization, for two samples each from the Dry Creek stock and the Vermilion River stock and one sample from the Lightning Creek stock (Table 2). Calculated pressures range from 2.7 to 5.0 kbar for the Dry Creek stock, 3.3 to 4.8 kbar for the Vermilion River stock, and 4.6 to 5.5 kbar for the Lightning Creek stock. The large range in pressures within a given pluton demonstrates the low precision of the calculated pressures. Crystallization depths inferred from these data are between 9 and 15 km, corresponding to mid- to upper crustal levels for crystallization. The contact aureole of the Dry Creek stock is as much as 2 km wide and that of the Lightning Creek stock is ~500 m wide and contains the assemblage quartz + biotite + muscovite + andalusite + plagioclase in pelitic country rocks. Assuming equilibrium was attained in the contact aureole, the maximum pressure for the stability of andalusite is ~3.5 kbar (Holdaway, 1971). This assemblage is typical of the hornblende-hornfels facies of contact metamorphism and agrees with pressure estimates determined from Al in hornblende, at temperatures of 400–600 °C (Turner, 1981).

Muscovite neoblasts are distinguishing features in the mylonitic western part of the Dry Creek stock. Fine-grained white mica in undeformed parts of the stock occurs only as local replacement of other phases. The neoblasts lie approximately parallel to S-surfaces in the mylonite, making up a few modal percent of the rock. Besides the muscovite neoblasts, scattered patches of fine-grained white mica occur in some biotite and feldspar crystals in the mylonite. A complex gradient is present in the age spectrum of the muscovite, with apparent ages from early gas release rising from 51 ± 3 Ma to 72 Ma in the latter part of the spectrum (Fig. 15e). Age gradients of this type may be the result of a mixture of two phases of white mica of different ages, as observed in other studies (Wijbrans and McDougall, 1986; McDougall and Harrison, 1988; Dunlap and others, 1991), although contamination of the muscovite with a small amount of biotite is possible. Textural evidence suggests that the fine-grained white mica crystallized later during the cooling history of the rock. A biotite age spectrum from the mylonite has apparent ages that rise smoothly from 54.6 ± 0.1 Ma to 56.7 ± 0.1 Ma corresponding to 95.9% gas released, which overlaps with the youngest ages of the muscovite spectrum.

We interpret the cooling age of the muscovite neoblasts to be the approximate age of mylonitization. An estimated minimum age of mylonitization is given by the total gas age of 69.4 Ma for the muscovite. A plateau age of 71.2 ± 0.5 Ma, corresponding to the last 64% of ^{39}Ar released at the highest temperatures gives an upper age limit on mylonitization (Fig. 15e). An inverse isochron of the muscovite step heating data has a very high mean square of the weighted deviates (MSWD = 148), making the total gas or plateau ages the preferred age of mylonitization. Laser analyses of groups of several grains (~1 mg) gave ages ranging from 65.2 ± 0.3 to 71.3 ± 0.3 Ma. From these data we interpret the time of mylonitization as ~71 to 69 Ma (Late Cretaceous, Maastrichtian), followed by cooling below ~300 °C (biotite T_c) in the early Eocene (~55 Ma). Modest ductility of quartz and a lack of recrystallization of either plagioclase or K-feldspar suggest temperatures of deformation compatible with synkinematic growth of the coarse muscovite neoblasts ($T_c \cong 350 \pm 50$ °C; McDougall and Harrison, 1988). Pressures from Al in hornblende indicate structural levels sufficient to allow ductile deformation.

Age and Significance of the Rock Lake and Hope Faults

In the Cabinet Mountains, granite intrusion and thrusting took place mainly during Late Cretaceous. The Moyie and Snowshoe thrust systems predate the Rock Lake fault, a later extensional structure. Similar age relations to thrusts and its normal-slip kinematics suggest that the Rock Lake fault may be tectonically related to the Hope fault.

Like those of the Hope fault, the age and kinematics of the Rock Lake fault are controversial. Harrison and others (1992) interpreted it as part of the east-directed Moyie thrust system despite its postthrusting field relations. On the basis of the spatial association between faulting and ore deposits in the Revett Formation, Lange and Sherry (1983) inferred that mineralization was syndepositional with respect to Belt strata, and involved northwest- to northeast-striking faults, including the Rock Lake fault. Structural evidence for a Precambrian precursor to the Rock Lake fault is lacking, however. Age relations established between thrust faults of the Moyie and Snowshoe systems and crosscutting relations between these thrusts and the Rock Lake fault indicate that major displacement on the Rock Lake fault occurred after ~69 to 71 Ma. Similarities in attitude and kinematics between the Rock Lake and Hope faults suggest an Eocene age for the latter. If the Hayes Ridge stock predates the Rock Lake fault as suggested by field rela-

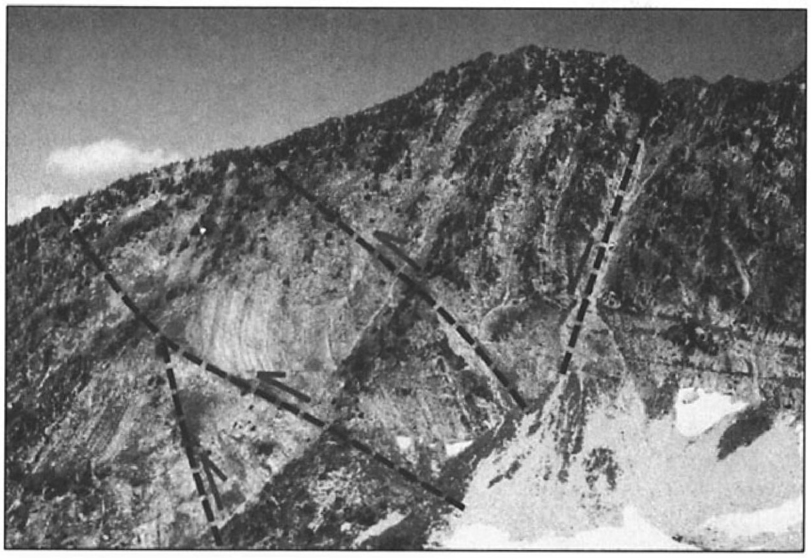

a

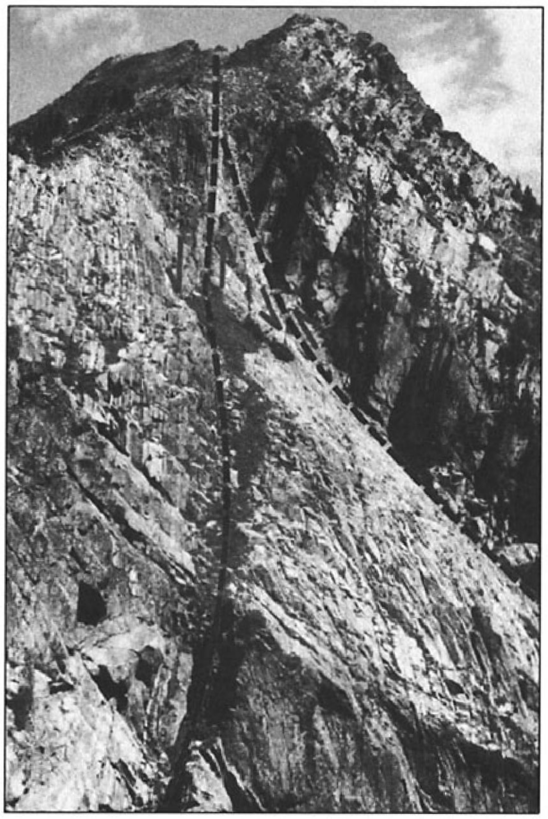

b

c

Figure 10. West-verging structures in the Rock Lake area: a and b are photographs taken looking north at structures present in cross section Figure 6b near Isabella Lake. (a) Imbricate thrusts of the Libby Lakes system in the footwall of the Snowshoe thrust; (b) minor normal faults that offset a strand of the Snowshoe thrust; (c) view toward the southeast of west-verging overturned anticline east of Rock Lake.

tions, then the Rock Lake fault is younger than the ca. 69 to 71 Ma Dry Creek stock mylonite and coeval with or younger than the $^{40}Ar/^{39}Ar$ cooling age of ~54 Ma determined for primary igneous muscovite for the Hayes Ridge stock (Fig. 15f, sample DC-45). We propose that the Hope and Rock Lake faults are part of the same extensional system that developed in the middle to late Eocene. Rapidly cooled K-feldspars from plutons in the footwall of the Hope fault at Vermilion River show accelerated cooling at ~38 Ma (Fillipone and others, 1992). The Hayes Ridge stock, which we interpret to be cut by the Rock Lake fault, experienced a final episode of rapid cooling at about 44 Ma, with a cooling rate of ~75 °C/m.y. (Fillipone, 1993). We attribute this rapid cooling to uplift along the Hope fault.

DISCUSSION

Previous studies of the relationship between magmatism and tectonism in the southwest Montana thrust belt have established that magmatism and thrusting overlapped in time (Robinson and others, 1968; Schmidt and Garihan, 1983; Harlan and others, 1988). Coeval Cretaceous thrusting and magmatism are now documented in the Cabinet Mountains (this study) and in parts of the southwest Montana thrust belt (Hyndman and others, 1988). Thrusting and magmatism in the Cabinet Mountains occurred in the Late Cretaceous, concurrent with imbricate thrusting and duplex development in the east. In northern Idaho, crystallization of part of the Kaniksu batholith in the northeast Priest River complex occurred around 94 Ma (Archibald and others, 1984), which is substantially older than movement on the Moyie thrust, the first major thrust east of the batholith. The White Creek batholith, dated at about 126 Ma (Wanless and others, 1968), cuts the Hall Lake fault in the northern part

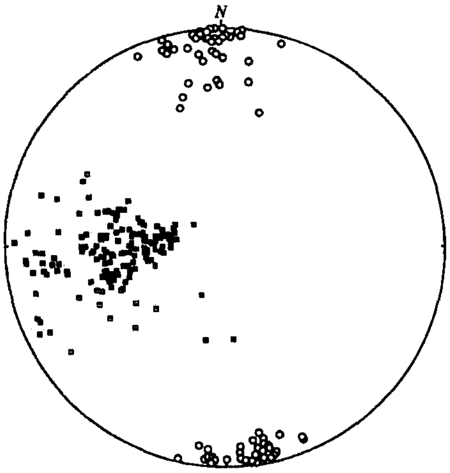

Figure 11. Lower hemisphere, equal-area projection of east-dipping cleavage, minor fold axes and bedding/cleavage intersection lineations associated with west-verging folds developed adjacent to the Snowshoe thrust in the Rock Lake area. Steep dips of cleavage and intersection lineations are attributed to deformation by movement on the Rock Lake fault.

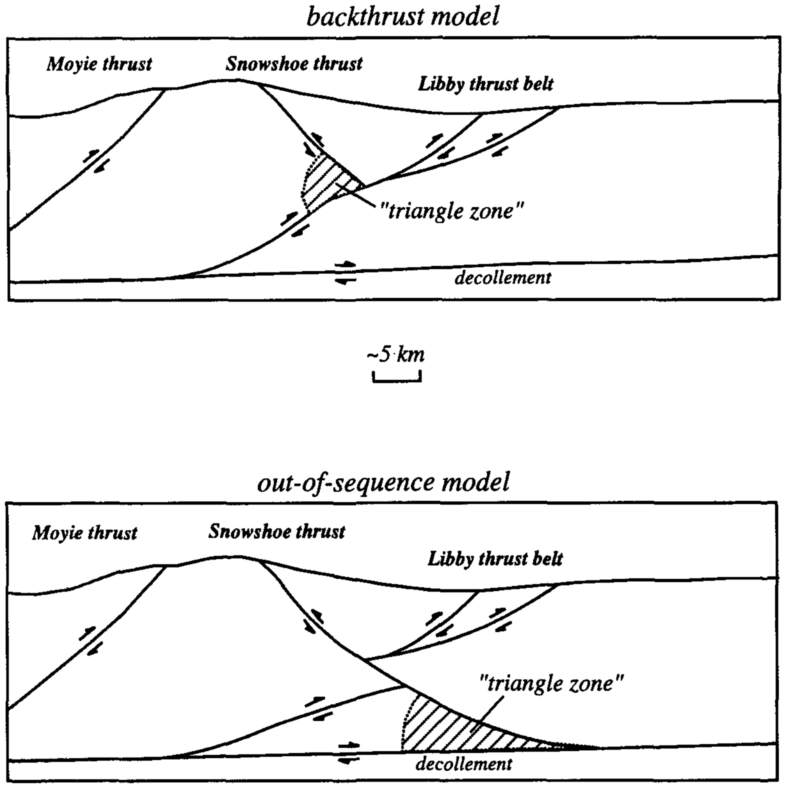

Figure 12. Diagrammatic kinematic interpretations of the Snowshoe thrust. (a) Option 1—Snowshoe thrust as a back thrust in the Libby thrust belt. The Snowshoe thrust could have developed coevally with the Libby thrust belt (LTB) at a ramp-flat junction or kink in the Libby thrust plane. Kinematically, this would make the Moyie thrust a later, out-of-sequence thrust (Morley, 1988) with respect to the LTB. (b) Option 2—Snowshoe thrust crosscuts the Libby thrust belt. Option 2 implies that the Snowshoe thrust may be out-of-sequence in relation to development of the LTB, thus creating a triangle zone (Jones, 1982) at the branch between the Snowshoe thrust and its potential junction with the regional décollement. This interpretation calls for imbricate thrusting in the LTB, followed by west-directed thrusting on the Snowshoe thrust, and finally, emplacement of the Moyie thrust sheet.

of the Purcell anticlinorium in southeast British Columbia, suggesting that thrusting there occurred earlier during the Cretaceous (Price, 1981). Hoy and van der Heyden (1988) showed that the St. Mary fault, part of a system of east- to southeast-directed reverse faults that includes the Moyie thrust in southeast British Columbia, was crosscut by a 94 Ma (U-Pb zircon) quartz monzonite stock. The St. Mary fault is thus either older than the Moyie thrust, or else the segment of the Moyie thrust we dated developed later than in the north.

Dip slip on the Moyie thrust diminishes from about 8 km in southeast British Columbia to about 4 km in the Cabinet Mountains in Montana. This decrease in slip on the Moyie thrust in Montana might be compensated by slip on the oppositely directed Snowshoe thrust and in the Libby thrust belt, both of which are absent in British Columbia. These north to south temporal and kinematic variations may account for the change in structural style between the Canadian and U.S. segments of the Purcell anticlinorium. The anticlinorium in British Columbia may have experienced greater combined Jurassic and Cretaceous shortening than it did in Montana (compare Price, 1981, with Harrison and others, 1980). The older ages of east-directed thrusts in southern British Columbia may also indicate that thrusting in the Purcell anticlinorium was diachronous, younging toward the south.

CONCLUSIONS

The Moyie thrust is interpreted from crosscutting relations as the youngest structure among a system of east-directed (Moyie thrust, Libby thrust belt) and west-directed (Snowshoe thrust) structures that developed during the Late Cretaceous (~71–69 Ma). Because thrusting was broadly coeval in the Cabinet Mountains, the Montana Disturbed belt (Hoffman and others, 1976), and parts of the southwest Montana thrust belt (Robinson and others, 1968; Perry and Sando, 1982; Harlan and others, 1988), the intervening area occupied by the Purcell anticlinorium may have acted as a linking structure between the hinterland and foreland. If the Purcell anticlinorium developed by up-to-the-

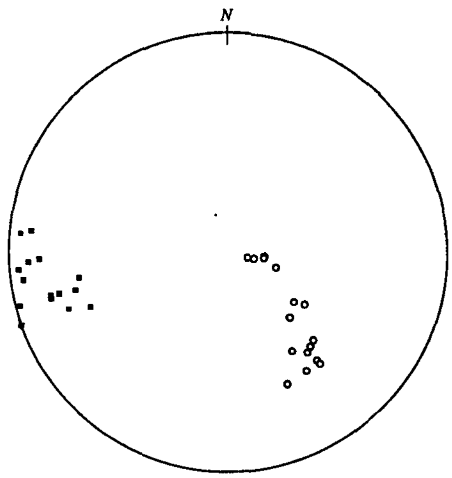

Figure 13. Structural data from the Rock Lake fault at St. Paul Pass, ~1 km north of Rock Lake (Fig. 5b, location 3).

TABLE 1. U-Pb ISOTOPIC DATA AND APPARENT AGES FOR THE DRY CREEK STOCK, SAMPLE DC-10

Weight (mg)	Size† (μm)	Concentration		Isotopic composition			Apparent ages (Ma)		
		Pb (ppm)	U (ppm)	$^{206}Pb/^{204}Pb$	$^{206}Pb/^{207}Pb$	$^{206}Pb/^{208}Pb$	$^{206}Pb^*/^{238}U$	$^{207}Pb^*/^{235}U$	$^{207}Pb^*/^{206}Pb^*$
0.38	30–45n	24.63	755	24,400	11.945	9.7	202.6 (0.6)	317.5 (1.0)	1278 (2)
0.81	45–63n	41.02	1,211	17,200	11.650	9.5	209.4 (0.6)	332.8 (1.1)	1320 (3)
0.36	63–100m	56.29	3,337	40,500	14.774	15.5	110.7 (0.3)	151.7 (0.5)	852 (3)
1.54	100–125n	36.09	1,232	32,000	11.962	10.3	183.1 (0.5)	290.2 (0.9)	1276 (3)
0.25	125–175m	46.04	2,492	26,500	14.230	15.1	120.7 (0.4)	170.0 (0.5)	925 (2)
0.10	145–350a	7.73	409	5,100	14.220	13.8	122.9 (0.4)	169.2 (0.7)	878 (5)

*Radiogenic Pb.

†m = magnetic separate; n = nonmagnetic separate; a = abraded in air abrasion device to approximately one-half of original diameter.

Note: Information about analytical techniques is provided in Gehrels (1990). Zircon fractions are divided into magnetic and nonmagnetic separates at 1.8 amps, 5° (side slope), and 15° (forward slope) on a Frantz isodynamic separator. Constants used: decay constant for $^{238}U = 1.55125 \times 10^{-10}$; decay constant for $^{235}U = 9.8485 \times 10^{-10}$; $^{238}U/^{235}U = 137.88$.

Uncertainties (in parentheses) are reported at the 95% confidence level. Isotopic compositions listed above have been adjusted only for Pb and U added with ^{205}Pb-^{233}U-^{235}U spike. In calculating concentrations and apparent ages the isotopic ratios are adjusted as follows:

(1) Mass-dependent correction factors of 0.14 (±0.06) %/AMU for Pb, and 0.04 (±0.04) %/AMU for UO_2.

(2) Pb ratios have been corrected for 0.010 (±0.005) ng blank with $^{206}Pb/^{204}Pb = 18.6\ (\pm 0.30)$; $^{207}Pb/^{204}Pb = 15.5\ (\pm 0.3)$; and $^{208}Pb/^{204}Pb = 38.0\ (\pm 0.8)$.

(3) U aliquot has been corrected for 0.001 (±0.001) ng blank.

(4) Common Pb remaining after correcting for blank Pb is interpreted to be initial Pb and is assigned a composition consistent with Stacey and Kramers (1975) with uncertainties of 2.0 for $^{206}Pb/^{204}Pb$, 0.3 for $^{207}Pb/^{204}Pb$, and 2.0 for $^{208}Pb/^{204}Pb$.

Analyses are by M. T. Smith and G. E. Gehrels, University of Arizona.

Sample location is indicated in Figure 5a (location 1).

east ramping of Belt strata during the Paleocene as suggested by Price (1981) and Archibald and others (1984), then structures toward the foreland should in general be younger than those in the hinterland. Our results indicate that episodes of thrusting in the hinterland and foreland occurred synchronously in the Late Cretaceous and were coeval with hinterland magmatism. Thus, the décollement linking these two regions apparently was established during the early stages of thrusting, as suggested by Yin and Kelty (1991). The foreland fold and thrust belt behaved as a wedge that experienced synchronous thrusting in its front and rear portions, suggesting that hinterland magmatism and thrusting was linked with thin-skinned thrusting farther onto the craton. These findings agree with predictions from mechanical models of thrusting, especially with respect to the wider spacing and steeper dips of thrusts expected in the thicker part of the thrust wedge, and to the presence of back thrusts (Davis and others, 1983; Chapple, 1978; Yin, 1993).

Throughout the hinterland of the Cordillera in the northwest United States and adjacent Canada, thrusting occurred near the locus of magmatism (Price, 1981; Hyndman and others, 1988), where magmatic heating may have contributed to thermal weakening of the lithosphere. By early Eocene, however, magmatism became associated with extensional tectonics (Parrish and others, 1988; Armstrong and Ward, 1991; Harms and Price, 1992). Extensional structures that crosscut thrusts in the hinterland developed after ~49 Ma, the age of the youngest rocks cut by the Hope fault (Hope sills; Fillipone and others, 1992). The Hope fault, southern Rocky Mountain trench fault system, and the Priest River and Bitterroot core complexes developed in the middle to late Eocene, when magmatism and extension were superposed on the foreland fold and thrust belt.

ACKNOWLEDGMENTS

This work forms part of a Ph.D. dissertation by J. Fillipone at the University of California, Los Angeles. We thank T. Mark Harrison for use of $^{40}Ar/^{39}Ar$ laboratory facilities at UCLA and Matthew Heizler for direction in the lab. George Gehrels and Moira Smith at the University of Arizona provided U-Pb analyses of the Dry Creek stock. Zell Peterman of the U.S. Geological Survey kindly made available the Rb-Sr data from the Dry Creek stock. Brian Gay and Karen Mitchell provided able assistance in the field. Russell Franklin of Kennecott Exploration (Spokane, Washington) offered insight into the geology of the Cabinet Mountains, provided samples of the Hayes Ridge stock, and kindly gave logistical support. We thank U.S. Forest Service District Ranger James Mershon (Cabinet District, Kootenai National Forest) for his interest in our project in the Cabinet

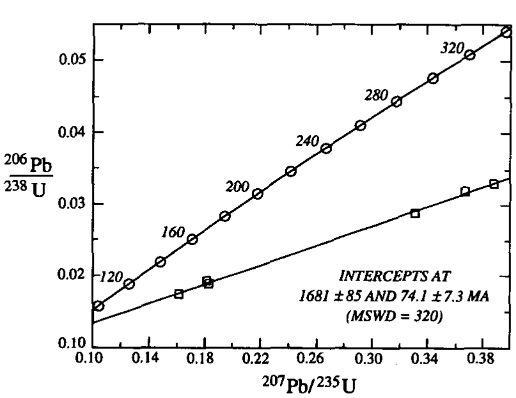

Figure 14. U-Pb concordia diagram of zircon analyses from sample DC-10. A concordia intercept age of 74.1 ± 7.3 Ma (95% confidence level) and an upper intercept age of ~1680 Ma indicate a significant inherited component in the zircons from this sample.

TABLE 2. CRYSTALLIZATION PRESSURES OF GRANITIC PLUTONS, CABINET MOUNTAINS, MONTANA AND IDAHO

Sample	Structural position	Pressure (kbar)
Dry Creek stock (DC-57)	Footwall of Moyie thrust	2.7–3.9
Dry Creek stock (DC-46)	Footwall of Moyie thrust	3.4–5.0
Vermilion River stock (VR-9)	Hanging wall of Moyie thrust	3.4–4.1
Vermilion River stock (VR-25)	Hanging wall of Moyie thrust	3.3–4.8
Lightning Creek stock (LC-34)	Hanging wall of minor thrust, above regional décollement	4.6–5.5

Note: Pressures calculated from the experimentally calibrated Al-in-hornblende geobarometer of Johnson and Rutherford (1989) for calcalkaline plutonic rocks. Locations of samples with respect to major thrust faults are mentioned.

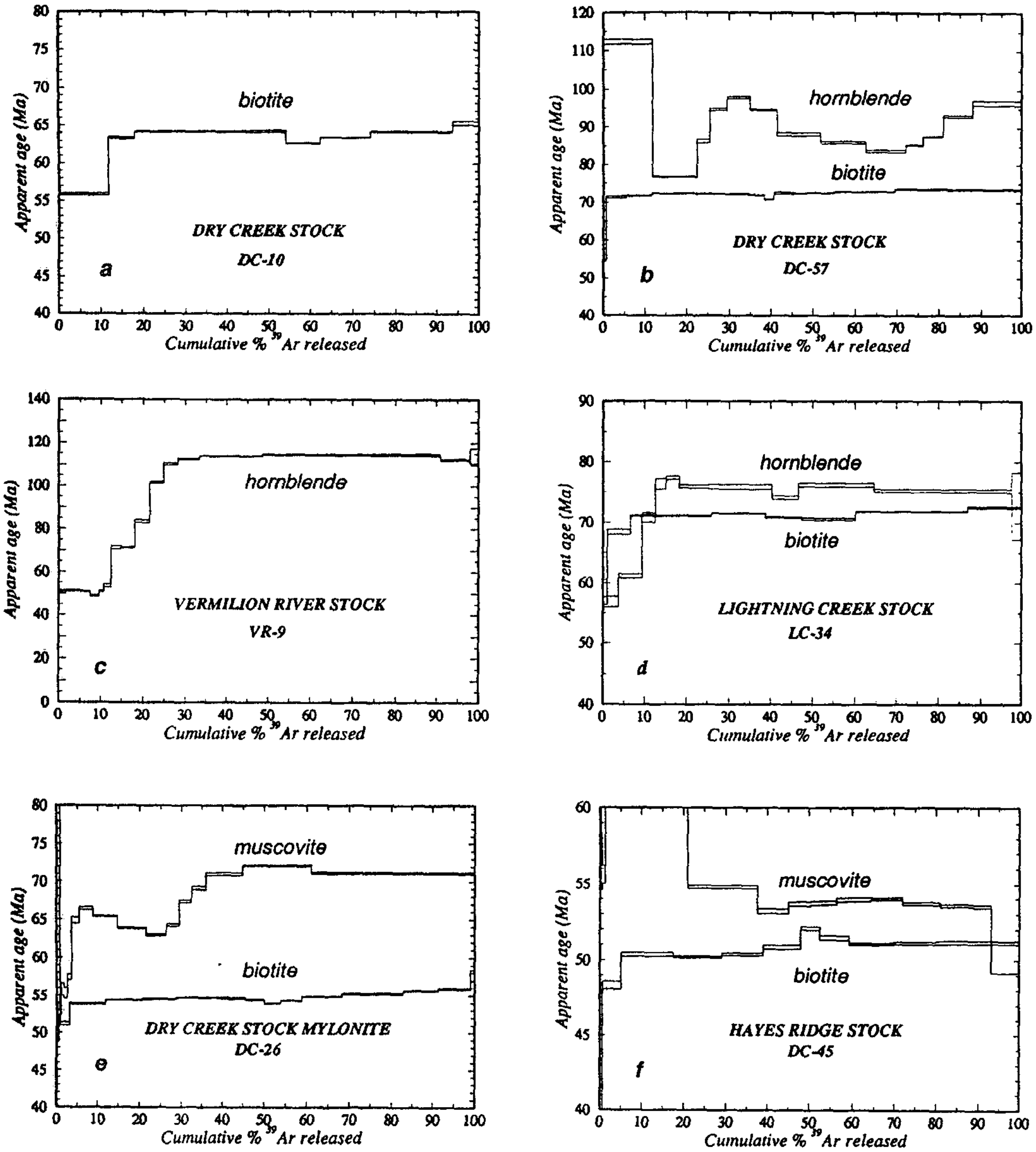

Figure 15. $^{40}Ar/^{39}Ar$ age spectra from the Cabinet Mountains (see Fig. 5 for sample locations): (a) Dry Creek stock, biotite (DC-10); (b) Dry Creek stock, hornblende and biotite (DC-57); (c) Vermilion River stock, hornblende (VRS); (d) Lightning Creek stock, hornblende and biotite (LC-34); (e) S-C mylonite of the Dry Creek stock, muscovite and biotite (DC-26); (f) Hayes Ridge stock, muscovite and biotite (DC-45).

Mountains Wilderness Area. Discussions with Mark Harrison and suggestions by Jim Dunlap helped us improve an earlier draft of this paper. Reviewers Donald W. Hyndman and Raymond A. Price keenly pointed out areas for improvement, and we gratefully acknowledge them. Associate editor Philippe Erdmer also provided helpful suggestions. Funding was provided through National Science Foundation Grant EAR 92-17525 to A. Yin, and grants to J. Fillipone from the Geological Society of America, American Association of Petroleum Geologists, and the Steven S. Oriel Memorial Research Fund of the Colorado Scientific Society.

REFERENCES CITED

Allmendinger, R. W., and Jordan, T. E., 1981, Mesozoic evolution, hinterland of the Sevier orogenic belt: Geology, v. 9, p. 308–313.

Archibald, D. A., Glover, J. K., Price, R. A., Farrar, E., and Carmichael, D. M., 1983, Geochronology and tectonic implications of magmatism and metamorphism, southern Kootenay Arc and neighbouring regions, southeastern British Columbia, Part I: Jurassic to mid Cretaceous: Canadian Journal of Earth Sciences, v. 20, p. 1891–1913.

Archibald, D. A., Krogh, T. E., Armstrong, R. L., and Farrar, E., 1984, Geochronology and tectonic implications of magmatism and metamorphism, southern Kootenay Arc and neighbouring regions, southeastern British Columbia, Part II: mid Cretaceous to Eocene: Canadian Journal of Earth Sciences, v. 21, p. 567–583.

Armstrong, R. L., 1988, Mesozoic and Cenozoic magmatic evolution of the Canadian Cordillera: Geological Society of America Special Paper 218, p. 55–91.

Armstrong, R. L., and Ward, P., 1991, Evolving geographic patterns of Cenozoic magmatism in the North American Cordillera: The temporal and spatial association of magmatism and metamorphic core complexes: Journal of Geophysical Research, v. 96, p. 13,201–13,224.

Armstrong, R. L., Taubeneck, W. H., and Hales, P. O., 1977, Rb-Sr and K-Ar geochronometry of Mesozoic granitic rocks and their Sr isotopic composition, Oregon, Washington and Idaho: Geological Society of America Bulletin, v. 88, p. 397–411.

Armstrong, R. L., Parrish, R. R., Reynolds, S. J., and Rehrig, W. A., 1987, Rb-Sr and U-Pb geochronometry of the Priest River metamorphic complex—Precambrian X basement and its Mesozoic-Cenozoic plutonic-metamorphic overprint, northeastern Washington and northern Idaho: Washington Division of Geology and Earth Resources Bulletin 77, p. 15–40.

Berthe, D., Choukroune, P., and Jegouzo, P., 1979, Orthogneiss, mylonite and non coaxial deformation of granites: The example from the South Armorican Shear Zone: Journal of Structural Geology, v. 1, p. 31–42.

Boyer, S. E., 1992, Geometric evidence for synchronous thrusting in the southern Alberta and northwest Montana thrust belts, *in* McClay, K. R., ed., Thrust tectonics: London, England, Chapman & Hall, p. 357–364.

Brown, R. L., and Tippett, C. R., 1978, The Selkirk fan structure of the southeastern Canadian Cordillera: Geological Society of America Bulletin, v. 89, p. 548–558.

Burchfiel, B. C., and Davis, G. A., 1975, Nature and controls of Cordilleran orogenesis, western United States: Extensions of an earlier hypothesis: American Journal of Science, v. 275-A, p. 363–396.

Bush, J. H., 1989, The Cambrian system of northern Idaho and northwestern Montana: Idaho Geological Survey Bulletin 28, p. 103–121.

Chapple, W. M., 1978, Mechanics of thin-skinned fold-and-thrust belts: Geological Society of America Bulletin, v. 89, p. 1180–1198.

Choukroune, P., Gapais, D., and Merle, O., 1987, Shear criteria and structural symmetry: Journal of Structural Geology, v. 9, p. 525–530.

Davis, D., Suppe, J., and Dahlen, F. A., 1983, Mechanics of fold-and-thrust belts and accretionary wedges: Journal of Geophysical Research, v. 88, p. 1153–1172.

Dunlap, W. J., Teyssier, C., McDougall, I., and Baldwin, S., 1991, Ages of deformation from K/Ar and $^{40}Ar/^{39}Ar$ dating of white micas: Geology, v. 19, p. 1213–1216.

Elliott, D., 1976, The motion of thrust sheets: Journal of Geophysical Research, v. 81, p. 949–963.

Fillipone, J. A., 1993, Tectonic and thermochronologic evolution of the Cabinet and Selkirk Mountains, northwest Montana and northern Idaho [Ph.D. dissert.]: Los Angeles, California, University of California, 341 p.

Fillipone, J. A., and Yin, A., 1993, Magmatism and denudation, a mechanism for linking extension across the northern Basin and Range province: Geological Society of America Abstracts with Programs, v. 25, p. 37.

Fillipone, J. A., Harrison, T. M., Sample, J. C., and Yin, A., 1992, Thermochronological evolution of the Hope and Moyie fault systems, NW Montana and NE Idaho: Geological Society of America Abstracts with Programs, v. 24, no. 6, p. 11.

Gehrels, G. E., 1990, Late Proterozoic–Cambrian metamorphic basement to the Alexander terrane on Long and Dall Islands, southeastern Alaska: Geological Society of America Bulletin, v. 102, p. 760–767.

Gibson, R., 1948, Geology and ore deposits of the Libby quadrangle, Montana: U.S. Geological Survey Bulletin 956, 131 p.

Gwinn, V. E., 1961, Geology of the Drummond area, central-western Montana: Montana Bureau of Mines and Geology Special Publication 21, Geologic Map No. 4.

Harlan, S. S., Geismann, J. Wm., Lageson, D. R., and Snee, L. W., 1988, Paleomagnetic and isotopic dating of thrust-belt deformation along the eastern edge of the Helena salient, northern Crazy Mountains basin, Montana: Geological Society of America Bulletin, v. 100, p. 492–499.

Harms, T. A., and Price, R. A., 1992, The Newport fault: Eocene listric normal faulting, mylonitization, and crustal extension in northeast Washington and northwest Idaho: Geological Society of America Bulletin, v. 104, p. 745–761.

Harrison, J. E., and Cressman, E. R., 1985, The Libby thrust belt and adjacent structures—New factors to consider in thrust tectonics of northwestern Montana: Geological Society of America Abstracts with Programs, v. 17, p. 223.

Harrison, J. E., and Jobin, D. A., 1963, Geology of the Clark Fork quadrangle, Idaho-Montana: U.S. Geological Survey Bulletin 1141-K, 38 p.

Harrison, J. E., and Schmidt, P. W., 1971, Geologic map of the Elmira quadrangle, Bonner County, Idaho: U.S. Geological Survey Geologic Quadrangle Map GQ-953.

Harrison, J. E., Kleinkopf, M. D., and Obradovich, J. D., 1972, Tectonic events at the intersection between the Hope fault and the Purcell trench, northern Idaho: U.S. Geological Survey Professional Paper 719, 24 p.

Harrison, J. E., Kleinkopf, M. D., and Wells, J. D., 1980, Phanerozoic thrusting in Proterozoic Belt rocks, northwestern United States: Geology, v. 8, p. 407–411.

Harrison, J. E., Griggs, A. B., and Wells, J. D., 1986, Geologic and structure maps of the Wallace 1° × 2° quadrangle, Montana and Idaho: U.S. Geological Survey Miscellaneous Investigations Series Map I-1509-A.

Harrison, J. E., Cressman, E. R., and Whipple, J. W., 1992, Geologic and structure maps of the Kalispell 1° × 2° quadrangle, Montana, and Alberta and British Columbia: U.S. Geological Survey Miscellaneous Investigations Series Map I-2267.

Hoffman, J., Hower, J., and Aronson, J. L., 1976, Radiometric dating of time of thrusting in the disturbed belt of Montana: Geology, v. 4, p. 16–20.

Holdaway, M. J., 1971, The stability of andalusite and the aluminum silicate phase diagram: American Journal of Science, v. 271, p. 97–131.

Hoy, T., and van der Heyden, P., 1988, Geochemistry, geochronology, and tectonic implications of two quartz monzonite intrusions, Purcell Mountains, southeastern British Columbia: Canadian Journal of Earth Sciences, v. 25, p. 106–115.

Hyndman, D. W., 1983, The Idaho batholith and associated plutons, Idaho and western Montana: Geological Society of America Memoir 159, p. 213–240.

Hyndman, D. W., Alt, D., and Sears, J. W., 1988, Post-Archean metamorphic and tectonic evolution of western Montana and northern Idaho, *in* Ernst, W. G., ed., Metamorphic and crustal evolution of the western United States (Rubey Volume 7): Englewood Cliffs, New Jersey, Prentice-Hall, p. 333–361.

Isacks, B. L., 1988, Uplift of the Central Andean Plateau and bending of the Bolivian Orocline: Journal of Geophysical Research, v. 93, p. 3211–3231.

Johnson, M. C., and Rutherford, M. J., 1989, Experimental calibration of the aluminum-in-hornblende geobarometer with application to Long Valley caldera (California) volcanic rocks: Geology, v. 17, p. 837–841.

Jones, P. B., 1982, Oil and gas beneath east-dipping underthrust faults in the Alberta foothills, *in* Powers, R. B., ed., Studies of the Cordilleran thrust belt: Denver, Colorado, Rocky Mountain Association of Geologists, p. 61–74.

Lange, I. M., and Sherry, R. A., 1983, Genesis of the sandstone (Revett) type of copper-silver occurrences in the Belt Supergroup of northwestern Montana and northeastern Idaho: Geology, v. 11, p. 643–646.

Lister, G. S., and Snoke, A. W., 1984, S-C mylonites: Journal of Structural Geology, v. 6, p. 617–638.

Marsh, B., 1982, On the mechanics of igneous diapirism, stoping, and zone melting: American Journal of Science, v. 282, p. 808–855.

McDougall, I., and Harrison, T. M., 1988, Geochronology and thermochronology by the $^{40}Ar/^{39}Ar$ method: New York, Oxford Monographs on Geology and Geophysics No. 9, 212 p.

McMechan, M. E., and Price, R. A., 1982, Transverse folding and superposed deformation, Mount Fisher area, southern Canadian Rocky Mountain thrust and fold belt: Canadian Journal of Earth Sciences, v. 19, p. 1011–1024.

Miller, D. S., Duddy, P. F., Hurford, A. J., and Naeser, C. W., 1984, Results of interlaboratory comparison of fission-track age standards: Fission Track Workshop, Nuclear Tracks, v. 10, p. 383–391.

Monger, J.W.H., Price, R. A., and Tempelman-Kluit, D. J., 1982, Tectonic accretion and the origin of the two major metamorphic and plutonic welts in the Canadian Cordillera: Geology, v. 10, p. 70–75.

Morley, C. K., 1988, Out-of-sequence thrusts: Tectonics, v. 7, p. 539–561.

Parrish, R. R., Carr, S. D., and Parkinson, D. L., 1988, Eocene extensional tectonics and geochronology of the southern Omineca Belt, British Columbia and Washington: Tectonics, v. 7, p. 181–212.

Paterson, S. R., Vernon, R. H., and Tobisch, O. T., 1989, A review for the identification of magmatic and tectonic foliations in granitoids: Journal of Structural Geology, v. 11, p. 349–363.

Perry, W. J., and Sando, W. J., 1982, Sequence of deformation of Cordilleran thrust belt in Lima, Montana region, *in* Powers, R. B., ed., Geologic studies of the Cordilleran thrust belt, Volume I: Rocky Mountain Association of Geologists, p. 137–144.

Platt, J. P., 1986, Dynamics of orogenic wedges and the uplift of high-pressure metamorphic rocks: Geological Society of America Bulletin, v. 97, p. 1037–1053.

Potter, C. J., Sanford, W. E., Yoos, T. R., Prussen, E. I., Keach, R. W., II, Oliver, J. E., Kaufman, S., and Brown, L., 1986, COCORP deep seismic reflection traverse of the interior of the North America Cordillera, Washington and Idaho: Implications for orogenic evolution: Tectonics, v. 5, p. 1007–1025.

Price, R. A., 1981, The Cordilleran foreland thrust and fold belt in the southern Canadian Rocky Mountains, *in* Price, N. J., and McClay, K. R., 1981, eds., Thrust and nappe tectonics: Geological Society (London) Special Publication No. 9, p. 427–448.

Price, R. A., 1986, The southeastern Canadian Cordillera: Thrust faulting, tectonic wedging and delamination of the lithosphere: Journal of Structural Geology, v. 8, p. 239–254.

Price, R. A., and Mountjoy, E. W., 1970, Geological structure of the Canadian Rocky Mountains between Bow and Athabasca Rivers—A progress report: Geological Association of Canada Special Paper No. 6, p. 7–25.

Rehrig, W. A., Reynolds, S. J., and Armstrong, R. L., 1987, A tectonic and geochronologic overview of the Priest River crystalline complex, northeastern Washington and northern Idaho: Washington Division of Geology and Earth Resources Bulletin 77, p. 1–14.

Rhodes, B. P., and Hyndman, D. W., 1988, Regional metamorphism, structure, and tectonics of northeastern Washington and northern Idaho, *in* Ernst, W. G., ed., Metamorphic and crustal evolution of the western United States (Rubey Volume 7): Englewood Cliffs, New Jersey, Prentice-Hall, p. 272–295.

Robinson, G. D., Klepper, M. R., and Obradovich, J. D., 1968, Overlapping plutonism, volcanism, and tectonism in the Boulder batholith region, western Montana: Geological Society of America Memoir 116, p. 557–576.

Schmidt, C. J., and Garihan, J. M., 1983, Laramide tectonic development of the Rocky Mountain foreland of southwestern Montana, *in* Lowell, J. D., ed., Rocky Mountains foreland basins and uplifts: Denver, Colorado, Rocky Mountain Association of Geologists, p. 271–294.

Scholten, R., 1982, Continental subduction in the northern U.S. Rockies: A model for back-arc thrusting in the western Cordillera, *in* Powers, R. B., ed., Geologic studies of the Cordilleran thrust belt, Volume I: Denver, Colorado, Rocky Mountain Association of Geologists, p. 123–136.

Simpson, C., and Schmid, S. M., 1983, An evaluation of criteria to deduce the sense of movement in sheared rocks: Geological Society of America Bulletin, v. 94, p. 1281–1288.

Smith, A. G., 1981, Subduction and coeval thrust belts, with particular reference to North America, *in* Price, N. J., and McClay, K. R., eds., Thrust and nappe tectonics: Geological Society (London) Special Publication No. 9, p. 111–124.

Stacey, J. S., and Kramers, J. D., 1975, Approximation of terrestrial lead isotope evolution by a two-stage model: Earth and Planetary Science Letters, v. 26, p. 207–221.

Stoffel, K. L., and five others, 1991, Geologic map of northeast Washington—Northeast quadrant: Washington Division of Geology and Earth Resources Geologic Map GM-39.

Turner, F. J., 1981, Metamorphic petrology: Mineralogical, field and tectonic aspects: New York, McGraw-Hill, 524 p.

Wanless, R. K., Loveridge, W. D., and Mursky, G., 1968, A geochronological study of the White Creek batholith, southeastern British Columbia: Canadian Journal of Earth Sciences, v. 5, p. 375–386.

Wells, J. D., Lindsey, D. A., and Van Loenen, R. E., 1981, Geology of the Cabinet Mountains Wilderness, Lincoln and Sanders Counties, Montana: U.S. Geological Survey Bulletin 1501.

Wijbrans, J. R., and McDougall, I., 1986, $^{40}Ar/^{39}Ar$ dating of white micas from an Alpine high-pressure metamorphic belt on Naxos (Greece): The resetting of the argon isotopic system: Contributions to Mineralogy and Petrology, v. 93, p. 187–194.

Winston, D., 1986, Belt Supergroup stratigraphic correlation sections showing general lithologies and history of formal usage: Montana Bureau of Mines and Geology Geologic Map Series No. 40.

Winston, D. W., 1989, A sedimentologic and tectonic interpretation of the Belt, *in* Middle Proterozoic Belt Supergroup, western Montana: 28th International Geologic Congress, Field Trip Guidebook T334, p. 47–69.

Yin, A., 1991, Kinematics of the Hope-Ninemile fault and its tectonic implications, northern Idaho and northwestern Montana: Geological Society of America Abstracts with Programs, v. 23, p. 111.

Yin, A., 1993, Mechanics of wedge-shaped fault blocks 1. An elastic solution for compressional wedges: Journal of Geophysical Research, v. 98, p. 14,245–14,256.

Yin, A., and Kelty, T. K., 1991, Structural evolution of the Lewis plate in Glacier National Park, Montana: Implications for regional tectonic development: Geological Society of America Bulletin, v. 103, p. 1073–1089.

Yoos, T. R., Potter, C. J., Thigpen, J. L., and Brown, L., 1991, The Cordilleran foreland thrust belt in northwestern Montana and northern Idaho from COCORP and industry seismic reflection data: American Association of Petroleum Geologists Bulletin, v. 75, p. 1089–1106.

Manuscript Received by the Society May 4, 1993
Revised Manuscript Received October 1, 1993
Manuscript Accepted October 20, 1993

Printed in U.S.A.